applied sciences

MDPI

Article

Development and Evaluation of a Fluctuating Plume Model for Odor Impact Assessment

Marzio Invernizzi [1,*], Federica Capra [1], Roberto Sozzi [2], Laura Capelli [1] and Selena Sironi [1]

[1] Department of Chemistry, Materials and Chemical Engineering "Giulio Natta", Politecnico di Milano, Piazza Leonardo da Vinci 32, 20133 Milan, Italy; federica.capra@mail.polimi.it (F.C.); laura.capelli@polimi.it (L.C.); selena.sironi@polimi.it (S.S.)

[2] Independent Researcher, 20133 Milan, Italy; robertosozzi50@gmail.com

* Correspondence: marzio.invernizzi@polimi.it

Featured Application: The dispersion model here presented can be a first approach for the definition of a simple screening model for odor impact assessment with non-constant peak-to-mean, in case Gaussian Plume model is fit to the aim.

Abstract: For environmental odor nuisance, it is extremely important to identify the instantaneous concentration statistics. In this work, a Fluctuating Plume Model for different statistical moments is proposed. It provides data in terms of mean concentrations, variance, and intensity of concentration. The 90th percentile peak-to-mean factor, R_{90}, was tested here by comparing it with the experimental results (Uttenweiler field experiment), considering different Probability Distribution Functions (PDFs): Gamma and the Modified Weibull. Seventy-two percent of the simulated mean concentration values fell within a factor 2 compared to the experimental ones: the model was judged acceptable. Both the modelled results for standard deviation, σ_C, and concentration intensity, I_c, overestimate the experimental data. This evidence can be due to the non-ideality of the measurement system. The propagation of those errors to the estimation of R_{90} is complex, but the ranges covered are quite repeatable: the obtained values are 1–3 for the Gamma, 1.5–4 for Modified Weibull PDF, and experimental ones from 1.4 to 3.6.

Keywords: odor impact assessment; dispersion modelling; peak-to-mean; concentration fluctuation; fluctuating plume model

Citation: Invernizzi, M.; Capra, F.; Sozzi, R.; Capelli, L.; Sironi, S. Development and Evaluation of a Fluctuating Plume Model for Odor Impact Assessment. *Appl. Sci.* **2021**, *11*, 3310. https://doi.org/10.3390/app11083310

Academic Editor: Ki-Hyun Kim

Received: 26 February 2021
Accepted: 1 April 2021
Published: 7 April 2021

1. Introduction

Odor is a property of a mixture of substances able to stimulate the olfactory sense. In the human nose, there are millions of receptors and the smell perception arises from the combination of the reactions of the nasal receptors to a wide range of odorous gases (H_2S, NH_3, VOCs, and more) [1,2]. Therefore, the main sources of environmental odors are the emissions of those odorous gases into the Planetary Boundary Layer (PBL) from industrial and agricultural activities [3–5]. Due to the proximity of residential centers to industrial areas, odor is one of the main causes of complaint to authorities [6,7].

In the PBL, like any other meteorological variable, the instantaneous concentration of odorous gases, more or less fluctuates, in time and space around to the local mean value, depending on the turbulence level of the atmosphere [8,9]. This is the reason why fluid dynamics researchers attribute to each PBL variable, and therefore also to the concentration of a passive scalar, the character of a stochastic variable completely defined by an appropriate Probability Density Function (PDF) [10–12]. Therefore, in order to completely know the statistics of the instantaneous concentration of a gas, it would be necessary to know its PDF or, equivalently, its infinite statistical moments, for each of

which, it is theoretically possible to write an appropriate partial differential equation describing its budget [8,9,12,13].

From a practical point of view, when interest is focused to Air Pollution and the related main pollutants (e.g., NO_2, CO, SO_2, O_3, PM_{10}, $PM_{2.5}$, and C_6H_6), the task is limited to the knowledge of the average concentration. Actually, for this purpose, models of various complexity are now available, both Eulerian [13,14] and Lagrangian [15].

Things are different when dealing with environmental odors. In this case, peaks concentration of a vast set of (odorous) substances mixed in the ambient air are conveyed to the human olfactory system through every respiratory act of extremely short duration, which can last the order of 5 s [16,17]. If the instantaneous concentration of these substances in the inhaled air exceeds a certain threshold, the individual perceives a sensation [18]. While usually odorous gases do not create direct toxicological effects on health [19,20], they cause discomfort and malaise, headache, nausea, joint pain, pain in the arms or legs and a feeling of fullness in the stomach [21]. In this case, both measurements and modelling predictions of the concentration of odorous gases should be aimed at identifying the statistics of the instantaneous concentration.

Starting from instantaneous concentration measurements gathered in a suitable averaging period (for instance 1 h), practical possibilities to identify the peak hourly concentration C_p are, for example:

- $C_p = C_m + \sigma$, where C_m is the hourly mean value and σ its standard deviation [22]
- C_p equal to the maximum value of the instantaneous concentration in the considered averaging period [23]
- As an appropriate p^{-th} percentile of the instantaneous concentration at each point of the spatial domain [24]

A historical scientific challenge was the objectification of the subjective sensation of odor [25]. For this reason, the measurement of odors requires specific methods [26,27]. There are many regulations for Air Pollution, but olfactory pollution is typically treated differently. As previously mentioned, the trend in space and time of the instantaneous concentration of a gaseous species is very irregular. For instance, the sensation of smell is perceived mostly in hours when the PBL turbulence is low and therefore the atmospheric stability is high, i.e., at evening and early morning [17,28]. In these situations, the use of an atmospheric dispersion model appears to be crucial [29–31]. As a matter of fact, the majority of environmental odor legislations around the world lean upon models [32,33]. The outputs of the dispersion models used in Air Pollution assessment and forecast are usually the hourly-mean concentrations C_m, but this information is not sufficient to describe completely the nature of an odor nuisance process [34,35]. To consider the variability of the ambient odor concentration within the period of 1 hour, a constant peak-to-mean factor C_p/C_m (also P/M) is usually provided by authorities [36–38]. As an example, the German legislation prescribes that all olfactory considerations of a modelling type, "Must be made considering an appropriate peak concentration". The Standard requires that the hourly average concentration obtained from the model is simply multiplied by a constant numerical factor equal to 4 [36,37]. Differently, all the regional guidelines present in Italy, suggest the value of 2.3 [38–40]. Unluckily, the experimental data show that a huge amount of physical phenomena have an effect on concentration fluctuations, demonstrating that the choice of a constant parameter is a very simplified approach [41]. Different simple methods for the calculation of this "peak-to-mean" factor can be found in literature; it is worth mentioning the constant peak-to-mean [36], the peak-to-mean variable only depending on atmospheric stability [42] and the one variable with stability and distance downwind the emission source [43,44]. Obtaining the sub-hourly percentile (and so the peak concentration) of a passive substance via dispersion model is not a trivial challenge. An alternative approach, available for Gaussian models is the consideration of recalculated lateral dispersion coefficients, in order to make them able to estimate ambient concentrations with averaging times shorter that 10 min [45,46].

However, the use of new models able to assess the mean concentration and variance, based on the physical laws describing the transport and dispersion in air of a substance, treated as a stochastic variable, appears the most recently debated methodology for the identification of peak concentrations (however defined, but linked to the statistical characteristics of the instantaneous concentration). In Ferrero et al. (2019) [47] an updated and exhaustive review of the modelling methods that can be used for odor modelling has been presented, and the most suitable methods to represent real situations seem to be those based on a Lagrangian framework. The most used philosophy to solve the problem of estimating a sub-hourly percentile is to hypothesize a priori a realistic PDF for the passive concentration. Experimental evidences show that, for this purpose, it is sufficient to consider a two-parameter PDF that asymptotically reduces to an exponential distribution near the source and a Log-Normal distribution at great downwind distances [44]. Weibull distribution and especially Gamma distribution own these adaptability features. Since a two-parameter distribution is completely known once the mean value and the variance are obtained, this closure hypothesis means that, to describe the concentration fluctuations, and therefore to determine the desired percentile, it is sufficient to reconstruct the mean and the concentration variance.

One of the most interesting model is the Fluctuating (or Meandering) Plume model, originally proposed in qualitative terms by Gifford (1959) [48]. In Luhar et al. (2000) [49], the logical evolution of this modelling philosophy over the years is shown and a version based on Lagrangian Particle Modelling is described in detail. Further works have been published about this topic [50–53]. Within these studies, a Lagrangian version of the Fluctuating Plume is proposed, which provides extremely realistic reconstructions of the instantaneous concentration statistics. Unlucky, the complexity of the models proposed hinders their application for regulatory or screening evaluations.

The work of Marro et al.(2015) [54], instead, studies the Fluctuating Plume in situations that can be modelled by a Gaussian Plume Model for the average concentration (horizontal homogeneity of meteorological and micrometeorological variables and flat and horizontally homogeneous soil). In fact, these conditions are rather artificial, but can be considered realistic when the ground is flat, and the meteorological conditions are horizontally homogeneous and stationary. Primary focus of that work was to verify how much such a model was able to reproduce the extensive set of experimental measurements obtained by Nironi et al. (2015) [55] in a wind tunnel in substantially neutral turbulence. The important result reached is a semi-analytical expression for the different moments (uncentered) of the instantaneous concentration that reproduces with good approximation the measurements obtained in Nironi et al. (2015).

Our work starts from the general conclusions reached by Marro et al. (2015), in order to obtain a Gaussian Plume Model for the average concentration and its variance, totally algebraic and simple enough to be useful for design purposes. Based on the knowledge of the values representing the mean and variance, the parameters defining the two-parameter PDF are known, with which it is possible to estimate the peak concentration, defined as an appropriate percentile, at every point in time and space of the considered simulation domain. In order to evaluate the performance of the proposed model, a comparison with the Uttenweiler field dispersion test was conducted [56]. The simplicity of this model makes it useful at least for screening purposes and, in situations with flat and horizontally homogeneous terrain and with horizontally homogeneous meteorology, also for regulatory purposes. Its limitation consists in considering only one active emitting source.

In Section 2, the Lagrangian theory of the Fluctuating Plume is initially presented, and from it a new stationary Gaussian Plume formulation is obtained for the average concentration of a generic odorous substance and for its variance, as well as the methodology to be used to obtain the peak concentration. Section 3 briefly presents the Uttenweiler experimental campaign specifically dedicated to the measurement of the average concentration and variance, which was used to verify the behavior of the

Gaussian Stationary Fluctuating Plume model here developed. In Section 4, the results obtained using the model developed to reconstruct the Uttenweiler experimental campaign are presented and discussed. Section 5 presents some conclusions.

The Gaussian stationary formulation obtained holds only if one emission source is active, but its use in situations of practical interest would require its multisource extension and this is not straightforward. If, in fact, for the average concentration the superposition of the effects holds, so it is not a priori for the variance and for the percentiles, since the turbulence of the PBL somehow correlates the different emission sources. This topic is currently still an open challenge and the Supplementary Material presents some considerations and possible practical solutions.

The purpose of the work described in this paper is to obtain a prototypal implementation of the theoretical model presented. Our aim is to obtain a preliminary test of the reliability and the usability of a simple and analytical model to estimate ambient peak concentrations, crucial for odor assessments. Only after a widespread experimental verification, the model will be worthy of a proper operative development, including an official implementation, releases, user's manual, and public distribution.

2. Model Development

2.1. Conceptual Bases of the Fluctuating Plume Model

When a passive scalar, like a tracer or odorous gas, from a point source is emitted, in reality, many instantaneous plumes are generated in sequence, each different from the other and irregularly shaped. Only considering their average, they make up the usual regular plume characterized by a progressive enlargement in downwind direction, proportional to the turbulence present in the PBL. If we focus our attention on a single instantaneous plume, we can clearly see that in the first phase of dispersion, near the source, the plume is coherent, narrow and meandering, mainly horizontally and, to a lesser extent, also vertically. The plume meandering, more accentuated near the source, progressively reduces downwind until it disappears: the meandering extent is inversely proportional to the plume's characteristic dimension. From this phenomenological evidence, the famous Fluctuating Plume Model proposed by Gifford (1959) was inspired, which was originally formulated more as a conceptual tool than a quantitative model. It should be pointed out that, in this context, the term meandering refers to the slow oscillation of a plume due to the eddies characterized by a length scale greater than the plume length scale and not to the slow horizontal oscillations of the mesoscale motion (the "submeso" motions) practically always present in the PBL and very evident in high stability [57–61].

Let us put a point source in position (0, 0, z_s) and a coordinate system centered in it (x along the direction towards the mean wind is blowing, the y horizontal and transverse to x and with the vertical z-axis) [48,62], and an averaging time of the order of the spectral gap (therefore of the order of the hour [8]). What we can see is a regular plume growing progressively with the distance downwind to the emission point, initially in linearly and subsequently in parabolic manner. Basically, in homogeneous and stationary turbulence, the average plume can be seen as a succession of slices (spreading disk), adjacent to each other in x direction, having flat surfaces in (y, z) and thickness $dx = Udt$, where U is the mean wind speed at the emission point and dt is an appropriate small time interval. The distribution of the average concentration in the plane (y, z), at least in first approximation, can be considered Gaussian and centered at points $y_s = 0$ and z_s (plume centroid).

If, instead, we subdivide the averaging time into a succession of shorter time steps, it is easy to imagine that the average plume is the result of the superimposition of ideally infinite instantaneous irregular plumes, whose barycenters no longer coincide with the x-axis, but meander around it. Further, in this case, the (instantaneous) plume can be seen as a series of slices placed one next to the other, but in each slice the concentration

distribution, always Gaussian in the y and z directions, is centered around a new centroid placed now at the transversal distance y_m and the vertical distance z_m.

Gifford (1959) used this idea to propose a simple conceptual model of a stationary Gaussian Meandering Plume. In Gifford's model, the concentration distribution within the instantaneous plume is strictly deterministic, being described in both y and z by a Gaussian distribution. This distribution is instead a stochastic variable, since the coordinates of the position of the centroid y_m and z_m are really stochastic variables due to the nature of the turbulent eddies in the PBL. However, Gifford's model does not account, neither directly nor explicitly, for the action of turbulent eddies of smaller dimensions than the plume. This dispersion, not considered by the Gifford's model, is named "relative dispersion" or "internal plume dispersion". In practice, if we were to sample at the point (x, y, z) at high frequency (i.e., at successive instants very close to each other), what we would obtain would be a sequence of instantaneous concentration c_i, each corresponding to a possible position of the centroid (y_m, z_m). These statistical realizations will be different from each other and, on average, they will give the average concentration C, which corresponds to the visible and overall result of an absolute dispersion process. Figure 1 reports a graphical example of the average and the instantaneous plume dispersion.

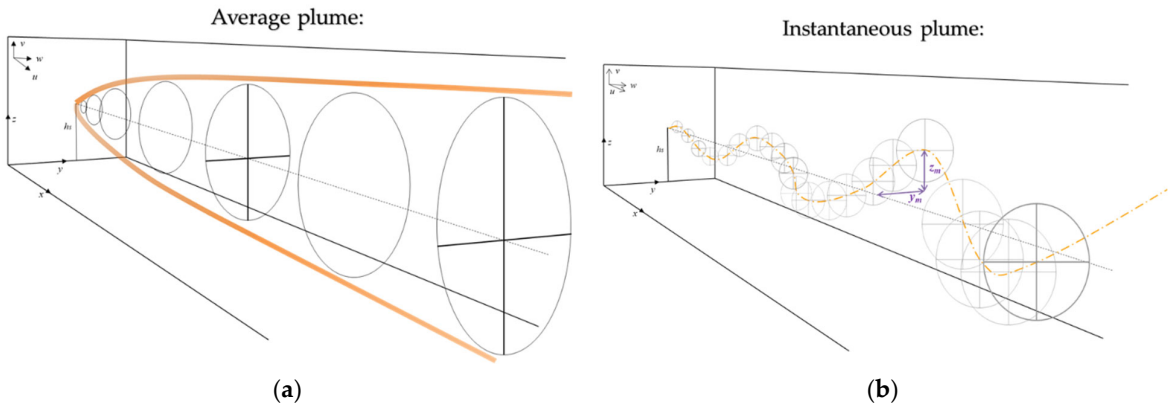

Figure 1. Graphical example of average plume (**a**) versus "single-disks" meandering plume (**b**).

Despite being very simplified, the Gifford's Fluctuating Plume model captures in an immediate fashion the phenomenology of the instantaneous dispersion of a passive substance in the PBL. Despite the fact that the ground reflections of instantaneous plumes in the original model are neglected, the biggest restriction of the model in its original formulation is that it assumes the transverse and vertical distribution of the concentration in an instantaneous plume to be deterministic (described by a Gaussian distribution) and not a stochastic process as the experimental evidence has confirmed. Further studies [63–65], more than 30 years after the model was proposed, extended Gifford's model to include fluctuations within the instantaneous plume. However, even though Gifford's Fluctuating Plume model was formulated on a predominantly phenomenological basis, in Yee and Wilson (2000) [65] it was shown to be theoretically justified, describing in a simple and immediate way the fact that the absolute (average) total dispersion of a passive substance in the turbulent PBL is the result of two different and practically independent stochastic processes: a dispersion due to the meandering of the plume centroid and a relative dispersion of the centroid itself. This conceptual model has been the key to a number of experimental campaigns aimed at highlighting the absolute dispersion of the plume, the relative dispersion, and the meandering of the centroid. In this regard it is worth referring to the works of Ma et al. (2005), Peterson et al. (1999), Peterson and Lamb (1995, 1992), and E. Yee et al. (1994) [66–70].

2.2. General Lagrangian Theory of the Fluctuating Plume Model

Let us consider a steady-state PBL of vertical extension z_i, one point source at (x_s,y_s,z_s) with constant emission rate Q and a horizontally homogeneous spatial domain. In these conditions, the fluctuating plume model can be reformulated more realistically in a purely Lagrangian framework [49–52]. The instantaneous concentration $c(x,y,z)$, if considering a continuous point source (with characteristic physical dimension σ_0) with position (x_s,y_s,z_s), is statistically described by the probability density function $p(x,y,z)$. Adopting the Fluctuating Plume philosophy, the dispersion can be considered as the combination (convolution) of two independent contributions (the floating part and the relative diffusion part). This distribution can be expressed by the convolution integral:

$$p(x,y,z) = \int_0^{\infty} \int_{-\infty}^{+\infty} p_{cr}(c;x,y,z,y_m,z_m) \cdot p_m(x,y_m,z_m) \cdot dy_m dz_m \quad (1)$$

where p_{cr} $(c; x, y, z, y_m, z_m)$ is the probability density function describing at the downwind distance x the dispersion of the generic passive with respect to the centroid of an instantaneous plume located at (y_m, z_m) (the relative dispersion) and p_m (x, y_m, z_m) is the probability density function that at x the centroid of the instantaneous plume has exactly those coordinates. Known the two probability density functions, we can calculate any n^{-th} moment of the instantaneous concentration. As a matter of fact, in a Lagrangian framework, a generic (uncentered) moment of order n will be expressed as

$$\overline{c^n}(x,y,z) = \int_0^{\infty} c^n \cdot p(c;x,y,z) \cdot dc \quad (2)$$

For example, the average concentration and the variance are expressed as

$$\overline{c}(x,y,z) = C(x,y,z) = \int_0^{\infty} c \cdot p(c;x,y,z) \cdot dc \quad (3)$$

$$\sigma_c^2 = \int_0^{\infty} c^2 \cdot p(c;x,y,z) \cdot dc - C^2 \quad (4)$$

and the concentration intensity as

$$i_c^2 = \frac{\overline{c^2} - \overline{c}^2}{C^2} = \frac{\sigma_c^2}{C^2} \quad (5)$$

Unlike Gifford (1959) and supported by experimental evidence [65,70], here it is assumed that the fluctuations inside the instantaneous plume can be statistically described using a predefined PDF p_{cr} $(c; x, y, z, y_m, z_m)$. Although Franzese (2003) [51] assumes this distribution as Log-Normal, Cassiani, and Giostra (2002), Luhar et al. (2000) and Mortarini et al. (2009) [51,52,54] hypothesize more realistically that the PDF is a Gamma distribution of the type:

$$p_{cr}(c;x,y,z,y_m,z_m) = \frac{\lambda^{\lambda}}{\overline{c}_r \Gamma(\lambda)} \cdot \left(\frac{c}{\overline{c}_r}\right)^{\lambda-1} exp\left[-\frac{\lambda c}{\overline{c}_r}\right] \quad (6)$$

where $\overline{c}_r$ is the mean concentration relevant to the instantaneous plume centroid, c the instantaneous concentration, and λ is defined as $\lambda = 1/i_{cr}^2$, where i_{cr} is the ratio of the standard deviation of the relative concentration σ_r to the mean relative concentration (see Section 2.6). On the other hand, the instantaneous plume centroid in x meanders stochastically [65] and this can be described by a probability density function $p_m(x, y_m, z_m)$ associated to the coordinates y_m and z_m. We can suppose the statistical independence of the transverse meandering from the vertical one, previously postulated by Gifford (1959), thus giving:

$$p_m(x,y_m,z_m) = p_{ym}(x,y_m) \cdot p_{zm}(x,z_m) \quad (7)$$

There are no theoretical considerations supporting this hypothesis; however, it is justified by the need to keep the model relatively simple, and it is not contradicted by any other experimental evidence.

2.3. Gaussian Fluctuating Plume Model for Statistical Moments (Marro's Model)

Following Marro et al. (2015), when the model deals with situations where the hypotheses underlying a Gaussian Plume Model are valid and the meteorology and turbulence are nearly steady-state and horizontally homogeneous, the horizontal meandering of the plume centroid can be described using a Gaussian PDF:

$$p_{ym}(x, y_m) = \frac{1}{\sqrt{2\pi}\sigma_{ym}} exp\left(-\frac{(y_m - y_s)^2}{2\sigma_{ym}^2}\right) \quad (8)$$

Indeed, in the vertical direction this homogeneity cannot exist, due to the action of the soil as a lower bound to dispersion and, in convective conditions, for the action of the PBL top z_i as upper bound. However, the simplest PDF that describes a realistic vertical meandering motion of the centroid of the instantaneous plume (principally in near neutral conditions) considers only the interaction with the ground, and therefore:

$$p_{zm}(x, z_m) = \frac{1}{\sqrt{2\pi}\sigma_{zm}}\left\{exp\left(-\frac{(z_m - z_s)^2}{2\sigma_{zm}^2}\right) + exp\left(-\frac{(z_m + z_s)^2}{2\sigma_{zm}^2}\right)\right\} \quad (9)$$

where y_s and z_s are the emission point coordinates. In these equations, σ_{ym} and σ_{zm} are the meandering dispersion parameters in horizontal and vertical direction and will be described in Section 2.6.

For a generic instantaneous plume with the centroid in position (y_m, z_m), described by PDF (8) and (9), the relative average concentration, $\overline{C_r}$, of the instant plume is

$$\overline{C_r} = \frac{Q}{U_m} p_{yr}(x, y, y_m) p_{zr}(x, z, z_m) \quad (10)$$

where U_m is the mean wind velocity at the height z_m and Q is the constant emission rate. For the quantification of $\overline{C_r}$, the explicit forms of the PDFs, statistically describing the relative transverse and vertical dispersion, are needed. The relative dispersion is fully represented by the following two relationships:

$$p_{yr}(x, y_m) = \frac{1}{\sqrt{2\pi}\sigma_{yr}} exp\left(-\frac{(y_m - y)^2}{2\sigma_{yr}^2}\right) \quad (11)$$

$$p_{zr}(x, z_m) = \frac{1}{\sqrt{2\pi}\sigma_{zr}}\left\{exp\left(-\frac{(z_m - z)^2}{2\sigma_{zr}^2}\right) + exp\left(-\frac{(z_m + z)^2}{2\sigma_{zr}^2}\right)\right\} \quad (12)$$

Further, in this case, a completely Gaussian relative transversal dispersion has been assumed, given the lack, in the hypotheses considered, of lateral barriers to the plume. Regarding the vertical relative dispersion, only the soil-bound has been considered. In order to make these PDFs effectively calculable, the standard deviations σ_{yr} and σ_{zr} must be known. Detailed explanation will be given in Section 2.6.

Taking all this into account and assuming an instantaneous concentration fluctuating according to a Gamma distribution, the n^{-th} moment of the concentration is obtained by placing the (1), (6), (7), (8), (9), and (10) in (2). The result is the complex relation (13), which cannot be solved analytically due to the presence of some integrals, which quantifies both the average value and any n^{-th} moment of the concentration. In order to effectively calculate the average concentration and the variance, which are indispensable parameters for the quantification of olfactory annoyance, it is first necessary to know the analytical relations that express the different variances present (those relevant to the meandering movement and those relevant to the relative dispersion) and the parameter i^2_{cr} necessary for the complete definition of the Gamma distribution (see Equation (6)).

$$\begin{aligned}\overline{c^n}(x,y,z) &= \int_0^\infty p_{zm}dz_m \cdot \int_{-\infty}^\infty p_{ym}dy_m \cdot \int_0^\infty c^n p_{cr}(c;x,y,z,y_m,z_m)\cdot dc = \\ &= \int_0^\infty p_{zm}dz_m \cdot \int_{-\infty}^\infty \frac{1}{\lambda^n}\frac{\Gamma(n+\lambda)}{\Gamma(\lambda)} \cdot \overline{c^n}\, p_{ym}\, dy_m = \\ &= \left(\frac{Q}{2\pi\sigma_{yr}\sigma_{zr}U_m}\right)^n \frac{1}{2\pi\sigma_{ym}\sigma_{zm}} \cdot \int_{-\infty}^\infty exp\left(-\frac{(y_m-y_s)^2}{2\sigma_{ym}^2}\right) \\ &\cdot exp\left(-\frac{n\cdot(y-y_m)^2}{2\sigma_{yr}^2}\right)\cdot dy_m \cdot \int_0^\infty \frac{1}{\lambda^n}\frac{\Gamma(n+\lambda)}{\Gamma(\lambda)} \\ &\cdot \left\{exp\left(-\frac{(z_m-z_s)^2}{2\sigma_{zm}^2}\right)+exp\left(-\frac{(z_m+z_s)^2}{2\sigma_{zm}^2}\right)\right\}\cdot \\ &\cdot \left\{exp\left(-\frac{(z-z_m)^2}{2\sigma_{zr}^2}\right)+exp\left(-\frac{(z+z_m)^2}{2\sigma_{zr}^2}\right)\right\}^n \cdot dz_m\end{aligned} \tag{13}$$

This is the main result obtained by Marro et al. (2015), but also the starting point for the development of our Steady State Gaussian Fluctuating Plume.

2.4. New Operational Gaussian Fluctuating Plume Model

The estimation of the olfactory annoyance requires to quantify the odorants peak concentration defined as an appropriate percentile C_p of the instantaneous concentrations collected within one hour: this can be achieved from a PDF able to describe the instantaneous concentration. If this PDF is a two-parameter distribution (such as a Log-Normal, a Weibull, or a Gamma), then the knowledge of the hourly spatial distribution of the mean concentration and the variance of the concentrations are sufficient to obtain the peak.

Our objective is, firstly, to obtain, from relation (13), for a generic n-th moment (uncentered), the appropriate relations for the average concentration C and for the variance of concentrations σ^2_C and, secondly, to simplify these relations by making them suitable for screening and regulatory use.

Equation (13), obtained by Marro et al. (2015), is totally general if the assumptions of applicability of a plume model are valid. Its practical applicability, however, is not straightforward, since it contains some integrals requiring a numerical solution. However, assuming the simple hypothesis that i_{cr} depends only on the downwind distance x [54], it is possible to analytically solve the integrals in (13) and finally obtain a totally algebraic relationship, even if rather complex, for the generic n-th moment (uncentered) of the instantaneous concentration:

$$\begin{aligned}\overline{c^n} &= \left(\frac{Q}{2\pi\sigma_{yr}\sigma_{zr}U_m}\right)^n \frac{\sigma_{yr}}{\left(n\sigma_{ym}^2+\sigma_{yr}^2\right)^{0.5}}\frac{\sigma_{zr}}{(n\sigma_{zm}^2+\sigma_{zr}^2)^{0.5}}\cdot\frac{1}{\lambda^n}\frac{\Gamma(n+\lambda)}{\Gamma(\lambda)}\cdot \\ &\cdot\ exp\left[-\frac{n(y-y_s)^2}{2\,(n\sigma_{ym}^2+\sigma_{yr}^2)}\right]\cdot\sum_{k=0}^{n}\left\{\binom{n}{k}\cdot exp\left[-\frac{(n-k)\cdot(z-z_s)^2}{2\,(n\sigma_{zm}^2+\sigma_{zr}^2)}\right]\cdot\right. \\ &\left.\cdot\ exp\left[-\frac{k(z+z_s)^2}{2\,(n\sigma_{zm}^2+\sigma_{zr}^2)}\right]\cdot exp\left[-\frac{(2z)^2k(n-k)}{2\,(n\sigma_{zm}^2+\sigma_{zr}^2)}\cdot\frac{\sigma_{zm}^2}{\sigma_{zr}^2}\right]\right\}\end{aligned} \tag{14}$$

where $\binom{n}{k}$ is the binomial coefficient $\frac{n!}{k!(n-1)!}$.

Considering *(n = 1)*, we obtain the Gaussian relationship for the spatial distribution of the mean concentration for a Gaussian plume:

$$\begin{aligned}C = \bar{c} &= \left(\frac{Q}{2\pi\sigma_{yr}\sigma_{zr}U_m}\right)\frac{\sigma_{yr}}{\left(\sigma_{ym}^2+\sigma_{yr}^2\right)^{0.5}}\frac{\sigma_{zr}}{(\sigma_{zm}^2+\sigma_{zr}^2)^{0.5}}\frac{1}{\lambda}\frac{\Gamma(1+\lambda)}{\Gamma(\lambda)}\cdot \\ &\cdot\ exp\left[-\frac{(y-y_s)^2}{2\,(\sigma_{ym}^2+\sigma_{yr}^2)}\right]\cdot\sum_{k=0}^{1}\left\{\binom{1}{k}\cdot exp\left[-\frac{(1-k)\cdot(z-z_s)^2}{2\,(\sigma_{zm}^2+\sigma_{zr}^2)}\right]\cdot\right.\end{aligned} \tag{15}$$

$$\cdot \; exp\left[-\frac{k(z+z_s)^2}{2\,(\sigma_{zm}^2+\sigma_{zr}^2)}\right]\cdot exp\left[-\frac{(2z)^2k(1-k)}{2\,(\sigma_{zm}^2+\sigma_{zr}^2)}\cdot\frac{\sigma_{zm}^2}{\sigma_{zr}^2}\right]\Bigg\}$$

Remembering the property of Euler's Gamma function $\Gamma(1+\lambda)=\lambda\cdot\Gamma(\lambda)$and that $\binom{1}{k}=1$ for $k=0, 1$ the relation (15) is reduced to:

$$C = \frac{Q}{2\pi\sigma_y\sigma_z U_m}\cdot exp\left[-\frac{(y-y_s)^2}{2\sigma_y^2}\right]\cdot\left[exp\left[-\frac{(z-z_s)^2}{2\sigma_z^2}\right]+exp\left[-\frac{(z+z_s)^2}{2\sigma_z^2}\right]\right] \quad (16)$$

i.e., the usual steady-state Gaussian relation for the mean concentration when only the ground reflection of a steady-state plume is considered.

In this relation, the parameters σ_y and σ_z of the absolute dispersion are set equal to $\sigma^2_y = \sigma^2_{ym} + \sigma^2_{yr}$ and $\sigma^2_z = \sigma^2_{zm} + \sigma^2_{zr}$, respectively. The λ parameter is not present in this equation, so C does not depend on the PDF: it depends only on parameters of the absolute dispersion.

Proceeding the analysis and setting $n = 2$, it is then possible to obtain the spatial distribution for the Gaussian plume uncentered second concentration moment:

$$\begin{aligned}\overline{c^2} = &\left(\frac{Q}{2\pi\sigma_{yr}\sigma_{zr}U_m}\right)^2\frac{\sigma_{yr}}{\left(2\sigma_{ym}^2+\sigma_{yr}^2\right)^{0.5}}\frac{\sigma_{zr}}{(2\sigma_{zm}^2+\sigma_{zr}^2)^{0.5}}\frac{1}{\lambda^2}\frac{\Gamma(2+\lambda)}{\Gamma(\lambda)}\cdot\\ &\cdot\; exp\left[-\frac{2(y-y_s)^2}{2\,(2\sigma_{ym}^2+\sigma_{yr}^2)}\right]\cdot\sum_{k=0}^{2}\left\{\binom{2}{k}\cdot exp\left[-\frac{(2-k)\cdot(z-z_s)^2}{2\,(2\sigma_{zm}^2+\sigma_{zr}^2)}\right]\cdot\right.\\ &\left.\cdot\; exp\left[-\frac{k(z+z_s)^2}{2\,(2\sigma_{zm}^2+\sigma_{zr}^2)}\right]\cdot exp\left[-\frac{(2z)^2k(2-k)}{2\,(2\sigma_{zm}^2+\sigma_{zr}^2)}\cdot\frac{\sigma_{zm}^2}{\sigma_{zr}^2}\right]\right\}\end{aligned} \quad (17)$$

But, $\frac{1}{\lambda^2}\cdot\frac{\Gamma(2+\lambda)}{\Gamma(\lambda)}=\frac{1}{\lambda^2}\cdot\lambda\cdot(1+\lambda)=\frac{1+\lambda}{\lambda}$, and setting $S_y^2=2\sigma_{ym}^2+\sigma_{yr}^2$ and $S_z^2=2\sigma_{zm}^2+\sigma_{zr}^2$, the second uncentered moment assumes the following analytical form:

$$\begin{aligned}\overline{c^2} = &\frac{1+\lambda}{\lambda}\frac{Q^2}{(2\pi U_m)^2\sigma_{yr}\sigma_{zr}}\frac{1}{S_yS_z}\cdot exp\left[-\frac{(y-y_s)^2}{S_y^2}\right]\cdot\\ &\cdot\left\{exp\left[-\frac{(z-z_s)^2}{S_z^2}\right]+exp\left[-\frac{(z+z_s)^2}{S_z^2}\right]+\right.\\ &\left.+\,2\cdot exp\left[-\frac{(z-z_s)^2}{2S_z^2}\right]\cdot exp\left[-\frac{(z+z_s)^2}{2S_z^2}\right]\cdot exp\left[-\frac{1}{2}\frac{(2z)^2}{S_z^2}\frac{\sigma_{zm}^2}{\sigma_{zr}^2}\right]\right\}\end{aligned} \quad (18)$$

Differently from the mean concentration, the second uncentered moment explicitly depends on the PDF parameter λ, which statistically describes the fluctuations of the instantaneous plume, and depends both explicitly and separately on the horizontal and vertical parameters that characterize the relative dispersion and meandering of the plume centroid.

Finally, the steady-state Gaussian Fluctuating Plume Model thus obtained consists of the following two equations: Equation (16) for the mean concentration and Equation (18) for its second moment. The concentration variance is equal to the second uncentered order moment minus the square of the mean concentration (see Equation (4)). Then, the standard deviation of the concentration is the root square of the concentration variance. This is the general form of the new steady-state Fluctuating Gaussian Plume Model used in the following.

2.5. Peak Concentration

Obtaining direct information about the concentration PDF is currently only possible by using extremely complex modelling techniques such as DNS (Direct Numerical Simulation) [71,72] and LES (Large Eddy Simulation) [73,74] modelling. However, these techniques, together with the complex techniques known as PDF methods [11], can only be applied to limited spatial domains and time intervals, far from the needs of applications

of practical interest. When, therefore, one needs to tackle the olfactory annoyance generated by an industrial source to the surrounding population over a whole year, it is necessary to choose different methods.

As it is well-known, full knowledge of the instantaneous concentration PDF would be achievable if its infinite relative statistical moments were all known. Realistically, only the budget equations for some of the statistical moments can be written and (numerically) integrated, and therefore it is necessary to introduce some empirical elements in the PDF identification process. In the Eulerian budget equation for a generic n^{-th} moment (e.g., the second one) there are terms dependent on the $n+1^{-th}$ moment [8], and therefore also simple integration of this equation needs the introduction of appropriate closures that parameterize these terms. Normally, when the interest is on the PDF of instantaneous concentrations c, as primary closure the hypothesis of a known a priori PDF, statistically describing c, is introduced. For example, if the PDF is a two-parameter distribution, it will be sufficient to know the field of the mean value and the concentration variance at each point of the calculation domain and at each moment.

Different studies [41,44,63,70,75–78] tackled the problem of identifying the type of PDF on the basis of various experimental measurements carried out in laboratory studies and in the atmosphere, but without reaching a decisive conclusion. The most common are the exponential, the clipped normal, Log-normal, Gamma, and Weibull. The Log-Normal is simple, but it is the stiffest [79]. In other works [80,81], exponential and clipped normal PDF are also supported. Currently, two of the most considered PDFs were used to calculate the peak concentration: the Gamma [24] and the Modified Weibull [82,83]. The PDF Gamma [84] is very complex, but it is the most adaptable: due to this, it is probably the most suitable for dealing with the statistics of concentration fluctuations. Anyway, what emerges is that the actual PDF tends to be exponential near the emission source, while at great distances downwind its shape is much more symmetrical, therefore similar to a Log-Normal. Interesting are the observations made by Nironi et al. (2015) [55] analyzing the numerous measurements obtained in the wind tunnel. Authors state, "these findings clearly support the existence of a universal function for the PDF of the concentration." Moreover, they show how the measures suggest the adoption, at least in first approximation, of a Gamma PDF type, precisely for its adaptability. It is worthy to remark, however, that also the Weibull distribution has similar characteristics.

Known at (x,y) the mean concentration $\bar{C}$, its variance σ^2_c and so the concentration intensity i_c, adopting as PDF a Gamma distribution or a Weibull distribution, it is then possible to obtain the n^{-th} percentile concentration C_n. According to the German legislation [36], the percentile of interest is the 90th: in this way, the 90th percentile of the sub-hourly concentration, C_{90}, can be considered as the peak concentration, C_p. Accordingly, the peak-to-mean can be defined as $R_{90} = \frac{C_p}{\bar{C}}$.

Even though the Gamma distribution seems to be the most realistic distribution, the fact that it does not allow the obtainment of the R_{90} in analytical form makes its practical use complex. Nevertheless, in the present study, Gamma PDF is considered as well, by setting a zeroing cycle for the calculation of the Gamma's R_{90}.

Much simpler is the use of the Weibull distribution. The two-parameter modified Weibull distribution is described as [83]:

$$p(c) = \lambda \cdot k \cdot (\lambda c)^{k-1} \cdot exp[-\lambda c]^k \quad (19)$$

where the scale parameter λ and the shape parameter k are given by

$$\lambda = \frac{\Gamma(1+\frac{1}{k})}{\bar{C}} \qquad k = \frac{1}{i^{1.086}} \quad (20)$$

and $\Gamma(\ldots)$ is the Gamma Function. After substitution, for calculating the R_{90} we used:

$$R_{90} = max\left[1.5\ ;\ 1.5 \cdot \left(\frac{(-\ln(0.1))^{i_c{}^{1.086}}}{\Gamma\left(1 + i_c{}^{1.086}\right)}\right)\right] \quad (21)$$

The interesting result obtained is represented by (21), which expresses the R_{90} ratio between the peak concentration C_p and the average concentration C, dependent on i_C.

If $i_C \to 0$, $k \to \infty$, thus $1/\Gamma(1+1/k) \to 1/\Gamma(1) = 1$, $(-\ln(1-p))^{1/k} \to 1$ and therefore R_P tends to 1, as is evident from the data in Figure 2 of [41]. Vice versa, if $i_C \to \infty$, then $k \to 0$; $1/\Gamma(1+1/k) \to 1/\Gamma(1) = 1$, $(-\ln(1-p))^{1/k} \to 0$ and $R_P \to 0$, as can be seen in the cited figure. Both when the intensity of concentration tends to zero and when it tends to infinity the value of R_{90} is finite and limited, and this implies that there is a value for i_C for which R_P is maximum. Numerically, we can see that for p equal to 90, 95, 98, 99 and 99.9 the maximum R_P value, for a standard Weibull distribution, is respectively 2.68, 4.67, 10.19, 18.76 and 142.70 connected with the i_C values 1.7, 2.3, 3.1, 3.7, 5.5. Therefore, whatever is the value of i_C, R_P never tends to infinity. Similar considerations can be made when a Gamma PDF is used.

2.6. Dispersion Parameters and Relative Concentration Intensity

According to the hypotheses on which the Fluctuating Plume is based, the relationships between the parameters describing the absolute dispersion of the plume (y, z), those that describe its relative dispersion (y_r, z_r) and the parameters that describe the meandering of the centroid of the instant plume (y_m, z_m) are

$$\sigma_y^2 = \sigma_{ym}^2 + \sigma_{yr}^2 \quad (22)$$

$$\sigma_z^2 = \sigma_{zm}^2 + \sigma_{zr}^2 \quad (23)$$

Referring to Marro et al. (2015) [54] for details and the Bibliography considered therein, we have that

- given the flight time t ($t = x/U_m$), the parameters σ_v and σ_w, the Eulerian standard deviations of the transverse and vertical component of motion, can be obtained from the Taylor theory of dispersion [85] as

$$\sigma_y^2 = \frac{\sigma_0^2}{6} + 2\sigma_v^2 T_{Lv}\left\{t - T_{Lv}\left[1 - exp\left(-\frac{t}{T_{Lv}}\right)\right]\right\} \quad (24)$$

$$\sigma_z^2 = \frac{\sigma_0^2}{6} + 2\sigma_w^2 T_{Lw}\left\{t - T_{Lw}\left[1 - exp\left(-\frac{t}{T_{Lw}}\right)\right]\right\} \quad (25)$$

where $T_{Lv} = \frac{2\sigma_v^2}{C_0\varepsilon}$ and $T_{Lw} = \frac{2\sigma_w^2}{C_0\varepsilon}$ are the Lagrangian decorrelation time scales, σ_0 is the characteristic source dimension (σ_0 is calculated as $\sigma_0 = \frac{D}{2.15}$ [86], where D is the internal diameter of the stack), $C_0 = 4.5$ is the Kolmogorov constant and, finally, ε is the mean turbulent kinetic energy dissipation rate.

- the longitudinal and vertical dispersion parameters for the relative dispersion can be expressed from the following relationships:

$$\sigma_{yr}^2 = \frac{(C_r/6) \cdot \varepsilon \cdot (t_s + t)^3}{\left\{1 + \left[\frac{(C_r/6) \cdot \varepsilon \cdot t^2}{2\sigma_v^2 T_{Lv}}\right]^{2/5}\right\}^{5/2}} \cdot exp\left[-\left(\frac{t}{T_{my}}\right)^2\right] + \sigma_y^2\left\{1 - exp\left[-\left(\frac{t}{T_{my}}\right)^2\right]\right\} \quad (26)$$

$$\sigma_{zr}^2 = \frac{(C_r/6) \cdot \varepsilon \cdot (t_s + t)^3}{\left\{1 + \left[\frac{(C_r/6) \cdot \varepsilon \cdot t^2}{2\sigma_w^2 T_{Lw}}\right]^{2/5}\right\}^{5/2}} \cdot exp\left[-\left(\frac{t}{T_{mz}}\right)^2\right] + \sigma_z^2\left\{1 - exp\left[-\left(\frac{t}{T_{mz}}\right)^2\right]\right\} \quad (27)$$

with the characteristic times $T_{my} = \alpha T_{Lv}$ and $T_{mz} = \alpha T_{Lw}$ considering a constant value of α equal to two. Taking the expression for σ^2_{yr} as example, it must respect two asymptotic conditions [51,87].

The first one holds when $t \to 0$; in this case, σ_{yr} takes the asymptotic form:

$$t \to 0 \qquad \sigma_{yr}^2 = \left(\frac{C_r}{6}\right) \cdot \varepsilon \cdot (t + t_s)^3 \tag{28}$$

where C_r is the Richardson–Obukhov constant equal to 0.8 and t_s is the time necessary for the plume to expand until it reaches dimension σ_0, so $t_s = [\sigma_0^2/(C_r\varepsilon)]^{1/3}$ (Monin and Yaglom, 2007).

The second one holds when $t \to \infty$ and in this case:

$$t \to \infty \qquad \sigma_{yr}^2 = 2 \cdot \sigma_v^2 \cdot T_{Lv} \tag{29}$$

The intensity of the relative concentration i_{cr} is a key parameter to fully define the Gamma probability distribution that characterizes the relative dispersion of the instantaneous plume, and therefore to actually obtain the various moments (including the average) through the relationship (14). However, this parameter has rarely been measured experimentally or numerically. Only few works available on the subject [55,88]. Given the scarce knowledge on the subject, a 1D model has normally been adopted for the estimation of i_{cr} relating this parameter only to the downwind distance. Marro et al. (2015) considered for i_{cr} both a 1D model and a 3D model; however, they have shown how only with a 1D model the relationship (14) can be analytically integrated. Since our goal is to obtain a plume model easy to use and suitable for carrying out preliminary impact assessments, supported also by the observations that a 1D model for i_{cr} leads to reasonably correct results [54], only the 1D models according to which $i_{cr} = i_{cr}(x)$ will be considered below.

Analysis [49] of experimental measurements [89,90] did not allow to univocally identify a relation for i_{cr} and operationally the cited work hypothesized to place $i_{cr} = 1$, so $\lambda = 1$. This assumption, not contradicted by the experimental evidence, implies the representation of the concentration fluctuations of the instantaneous plume as an Exponential distribution because a Gamma distribution is reduced to it when $\alpha = 1$. In practice, this means that at great distances from the emission all concentration fluctuations depend on the internal fluctuations of the instantaneous plume and meandering is negligible. In the light of the experimental evidence considered, this assumption for i_{cr} while being realistic was not completely satisfactory, although from the analyses made in the work cited this simple model for i_{cr} leads to a reasonably limited error.

Crucial at this regard are the measurements made inside a wind tunnel in near-neutral conditions [55]. Based on them, the authors developed a new 1D model that makes i_{cr} depend on the normalized downwind distance $\xi = x/z_i$, (z_i is the PBL top) according to

$$i_{cr} = \xi \frac{p_1\xi^2 + p_2\xi + p_3}{\xi^3 + q_1\xi^2 + q_2\xi + q_3} \tag{30}$$

where the coefficients p_1, p_2, p_3, q_1, q_2, q_3 depend on the height of the source, its characteristic dimension σ_0 and the vertical extension of the PBL. The experimental measurements of refer to three different types of sources [55]. In applications related to olfactory annoyance it is recurring to consider low source without buoyancy. Accordingly, it would seem appropriate to use the lower-level source (LLS) coefficients in the model here developed. The values of the coefficients are indicated in Table 1.

Table 1. Coefficients to calculate i_{cr} with Equation (30).

	p_1	p_2	p_3	q_1	q_2	q_3
LLS [55]	0.35	−0.65	5.97	2.50	−0.55	1.20

3. Materials and Methods

3.1. Software Implementation

The model here presented has been implemented in Matlab R2019b. The use of a Matlab code was due to a fast implementation of this prototypal approach.

The code was divided into the following different sections:

- Meteorological and micrometeorological input data
- Emission source data
- Calculation of average concentration
- Calculation of concentration standard deviation and concentration intensity
- Peak percentile calculation (with a PDF-dependent choice, Gamma, or Modified-Weibull).

The calculation domain was fixed as a square of 800 m × 800 m dimension, with a mesh grid of 10 m.

For the calculations, a laptop computer with 4 parallel processors, 1.8 GHz CPU and 16 GB RAM was used. The computational time needed of each trial was dependent on the chosen PDF: for the Modified Weibull it was about 1 s, while for Gamma, which needs a zeroing for the calculation of R_{90}, it was 5 s.

3.2. Uttenweiler Field Experiment

In this paragraph, we only provide a short description of the field dispersion experiment, with the aim to make the understanding of the results easier. Further details regarding the experimental campaign (e.g., chemical analysis) are extensively described in the field test report [56]. The campaign was conducted in a pre-existing pig farm in three different days: 12 and 13 December 2000 and 31 October 2001. The farm is located outside the small village Uttenweiler, 20 km west of the city of Bielberach (48.136° N, 9.652° E) in Germany. The surrounding area is mostly flat and has only slight elevations and nearly congruent with the validity hypotheses of a Gaussian Plume Model. This farm consists of the pig barn and the feed processing room. These are two buildings with a height of 7.7 and 10.6 m, respectively. The gas tracer, sulphur hexafluoride (SF_6) were continuously emitted by a single point source on the smaller building. It was at 8.5 m above the ground level, and it was connected to the internal ventilation system. The column was the union of three shafts (338 cm × 107 cm) guided into one of area 1.2 m^2. 14 trials were performed, named in alphabetical order from B to O: the experiment A was an attempt. In the lee of the building, one (experiments I to L) or two receptor transepts (experiments A to H) were arranged, perpendicular to the direction of wind. Five to six measurement point are posed on each of these crossbars; each test site had an air sampler to record the SF_6 concentrations averaged over the measurement period of 10 min. Fast-response concentration measurements of SF_6 were also taken. They were carried out with a sampling rate of 0.1 Hz at two receptors, and then analyzed by gas chromatography. In the south-southwest region under consideration, at 150 m from the source and a height of 3.5 m, an ultrasonic anemometer (USAT) was placed. It was operated with a frequency of 10 Hz. The ultrasonic anemometer/thermometer data were analyzed and averaged over 30 min according to methodology normally used by Eddy Covariance [91]. Wind direction and wind speed were also recorded by means of a cup anemometer placed at 10 m above the ground level. During the experiments of 31 October 2001 the meteorological column broke down, so the measurements were carried out on an auxiliary shaft at a height of 2 m. The measurement points are identified using an acronym: T for "Traverse" that represents the crossbar, and P for "Proband" that represents the subject that occupies the point where the measurements take place; T and P are followed by a number that indicates which of the two crossbars and which of the twelve positions on the crossbars.

3.3. Meteorological Data Setting

Eleven experiments have been considered, B-L: shortcomings in the acquirement of sonic input data for the trials M, N, and O made the evaluation for these datasets not

reliable. Particular attention, by the authors of the test, was paid to carry out the field trials with a stable/neutral atmosphere. In these conditions, the horizontal meandering effect can cause problems to describe the intermittency naturally present at the transversal limits of the plume [46]. Moreover, Gaussian models are not able to consider in an efficient way the horizontal meandering naturally present in nature. As evidence of this phenomenon, there is a large range of angles of wind direction measured by the sonic anemometer during every trial (Table 2). In order to overcome two possible problems, it was decided to do a data tuning for the wind direction. The first reason was that the mean concentration data, for this field experiment, are available on the average time of ten minutes and not of an hour (which is the standard averaging time for a simple Gaussian model). The second and most important reason is that the aim of this work was not the test of the mean concentration, but to provide a simple way to assess of σ_c, I_c and R_{90}. Therefore, it was necessary to obtain mean concentration values as much consistent as possible.

Table 2. Summary of the trials considered of Uttenweiler experiments and related meteorological conditions. σ_u, σ_v, σ_w: standard deviation of along-wind, crosswind, and vertical wind velocity components; u*: surface friction velocity.

Experiment	Date	Release Time		SF_6 Emission Rate	σ_u	σ_v	σ_w	u*	Wind Speed	Wind Direction	Wind Direction Range
		Start	End	(g/h)	(m/s)	(m/s)	(m/s)	(m/s)	(m/s)	(°)	(°)
B	12 December 2000	13:00	13:10	121.7	0.393	0.368	0.257	0.192	3.9	210	205–222
C	12 December 2000	14:10	14:20	121.7	0.427	0.436	0.306	0.198	4.6	220	214–238
D	12 December 2000	14:45	14:55	121.7	0.294	0.305	0.221	0.14	2.5	237	222–246
E	13 December 2000	12:00	12:10	121.7	0.968	0.946	0.624	0.365	7.9	246	238–267
F	13 December 2000	13:05	13:15	121.7	0.77	0.762	0.489	0.321	6.8	244.5	217–255
G	13 December 2000	13:50	14:00	121.7	0.738	0.725	0.496	0.306	6.5	242	233–258
H	13 December 2000	15:10	15:20	121.7	0.533	0.531	0.369	0.238	2.7	236	225–257
I	31 October 2001	11:40	11:50	225.5	0.792	0.762	0.504	0.346	5.4	222	208–237
J	31 October 2001	12:00	12:10	225.5	0.743	0.702	0.492	0.337	5.8	225.5	211–235
K	31 October 2001	13:40	13:50	225.5	0.688	0.674	0.454	0.295	4.5	226	206–234
L	31 October 2001	14:05	14:15	225.5	0.656	0.617	0.423	0.274	5.2	232	216–236

3.4. Performance Evaluation

In order to evaluate the reliability of the model, in a simplified and analytical way, it was decided to calculate some statistical indicators [92–95]:, mean bias (MB), normalized mean bias (NMB), root mean squared error (RMSE), normalized mean squared error (NMSE), index of agreement (IOA) and the fraction of predictions within a factor or two (FAC2). The following equations report the calculation methods:

$$MB = \frac{1}{N}\sum_{i=1}^{N} E_i = \bar{M} - \bar{O} \tag{31}$$

$$NMB = \frac{\sum_{i=1}^{N}(M_i - O_i)}{\sum_{i=1}^{N} O_i} = \frac{\bar{M}}{\bar{O}} - 1 \tag{32}$$

$$RMSE = \sqrt{\frac{1}{N}\sum_{i=1}^{N}(M_i - O_i)^2} \tag{33}$$

$$NMSE = \frac{\frac{1}{N}\sum_{i=1}^{N}(M_i - O_i)^2}{\bar{P}\bar{O}} \tag{34}$$

$$IOA = 1 - \frac{\sum_{i=1}^{N}(M_i - O_i)^2}{\sum_{i=1}^{N}(|M_i - \bar{O}| + |O_i - \bar{O}|)^2} \tag{35}$$

$$FAC2: 0.5 \leq \frac{M_i}{O_i} \leq 2 \quad (36)$$

where M_i is the single modelled value and O_i is the single observed value. All these parameters have ideal values: MB = 0, NMB = 0, $RMSE$ = 0; $FAC2$ = 1; IOA = 1. We also used regression lined scatter and quantile–quantile plots [96].

4. Results and Discussions

4.1. Raw Data Processing

The first step was the elaboration of input data. The meteorological conditions, micrometeorological data and emission rates, the considered trials, and the meteorological conditions for each trial, are reported in Table 2. Due to the considerations reported in Section 3.3, the penultimate column of Table 2 shows the wind direction that has been used for the simulations. As reported, the chosen values are fully within the range of wind directions measured over the 10 minutes of each trial.

The second step was to elaborate the fast-response ambient concentration data (Table 3). R_{90} was calculated from the ratio of the 90th percentile (C_{90}) of the fast-response concentrations and the mean concentration. The 90th percentile was obtained considering the extremes of the series. To make the elaboration of the raw data reported in Table 3, a graph is presented (Figure 2). In this graph it is possible to compare the values of C_m (blue bar), 90th percentile (brown bar) and C_{max} (yellow bar) reported in (μg/m³) for every fast-response concentration point of measurement. The colored columns show the relationship between the three variables. For B T1P5, D T1P3, and D T2P3, the values are very low compared to the scale of the other points. Their values are anyway readable in Table 3.

Table 3. For every fast-response point of measurement, mean concentration, peak concentration, standard deviation of concentration, intensity of concentration, 90th percentile concentration and R_{90} are reported. The receptors are indicated as TP, where T is the crossbar and P represents the subject which occupies the point where the measurements take place. The numbers indicate which of the two transvers and which of the twelve positions.

Trial	Receptor	C_m	C_{max}	σ_c	I_c	C_{90}	R_{90}
		(μg/m³)	(μg/m³)	(μg/m³)		(μg/m³)	
B	T1P5	0.01	0.09	0.02	1.98	0.0	3.1
	T2P4	1.13	7.36	1.76	1.56	3.7	3.2
C	T1P5	8.64	27.02	6.63	0.77	18.4	2.1
	T2P4	9.13	16.67	3.54	0.39	13.2	1.4
D	T1P3	0.01	0.04	0.01	1.60	0.0	3.3
	T2P3	0.02	0.04	0.02	0.85	0.0	1.9
E	T1P3	9.30	30.91	7.03	0.76	18.0	1.9
	T2P2	2.53	12.17	3.54	1.40	8.0	3.2
F	T1P2	13.70	36.39	8.75	0.64	25.1	1.8
	T2P2	6.79	16.92	4.37	0.64	12.8	1.9
G	T1P2	15.69	41.32	11.66	0.74	29.9	1.9
	T2P2	7.02	17.40	4.25	0.61	13.3	1.9
H	T1P4	3.41	36.15	7.40	2.17	11.0	3.2
	T2P3	5.44	21.72	6.33	1.16	15.0	2.7
I	T1P4	6.18	28.66	6.86	1.11	16.0	2.6
	T1P9	4.58	31.52	7.46	1.63	16.4	3.6
J	T1P4	3.24	26.29	5.92	1.83	6.9	2.1
	T1P8	8.47	36.09	8.63	1.02	20.1	2.4
K	T1P4	6.27	36.57	7.77	1.24	14.9	2.4
	T1P9	5.56	34.08	7.55	1.36	14.5	2.6

L	T1P4	0.76	8.15	1.15	1.52	1.5	2.0
	T1P9	19.81	37.18	8.82	0.45	31.1	1.6

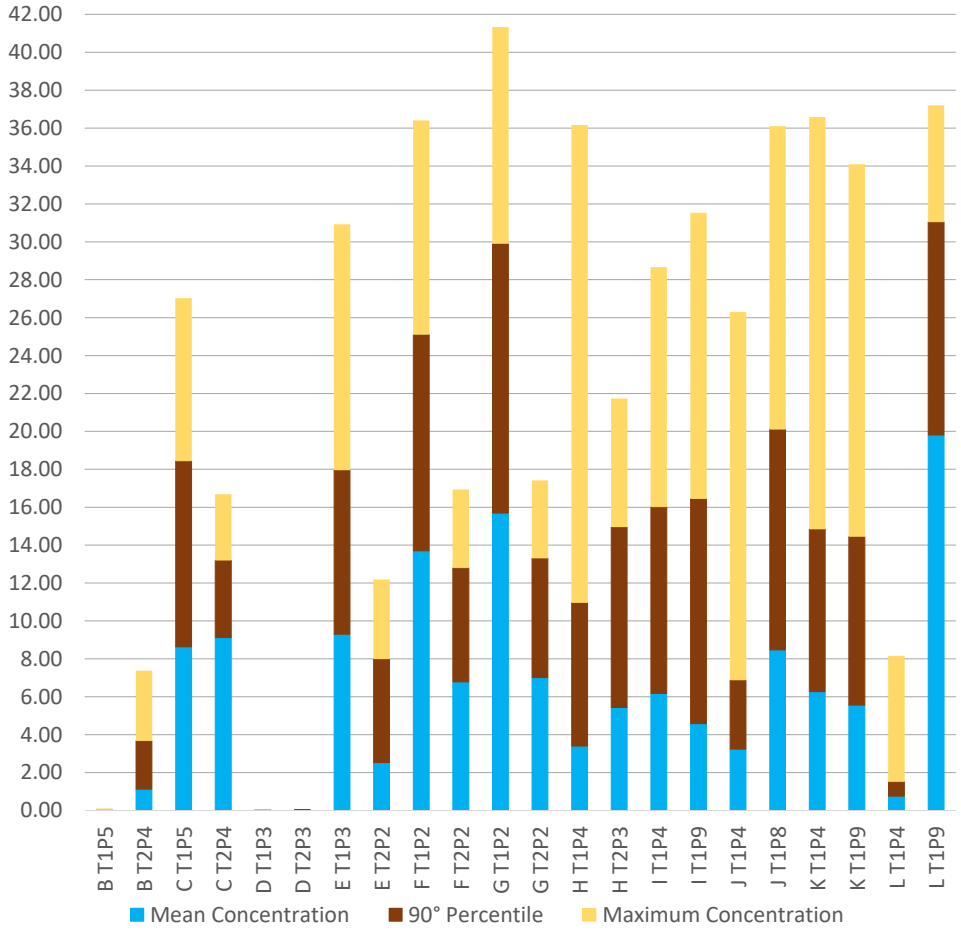

Figure 2. C_m, C_{90}, and C_{max} for every fast-response concentration point of measurement. On the *y*-axis, concentration values in µg/m3 are displayed, while on the *x*-axis all the fast-response receptors are reported. The receptors are indicated as a capital letter that represents the experiments and then T/P, where T is the crossbar and P represents the position where the measurement take places. The numbers indicate which of the two transvers and which of the 12 positions. For example, in B T2P4, the value of C_m is 1.13 µg/m^3, C_{90} is 3.7 µg/m^3, and C_{max} is 7.36 µg/m^3.

4.2. Mean Concentration

The first result obtained from the model is the average concentration, obtained with Equation (16). C_m values were calculated for each sampling position of each crossbar, for each trial. A total of 132 values were collected from the model. These values were compared with experimental 10-min data measurements. As mentioned in the field experiment document [56], measurements taken from deflated bag were considered unreliable and were removed from the comparison. To evaluate the quality of the model, performance parameters and some graphs are presented. Table 4 shows the results obtained from the performance evaluation: it is worth to remark that 72% of the values lies within a factor of 2 of the observations (FAC2). Moreover, parameters like MB and NMB are very close to the ideal zero value.

Table 4. Parameters for the performance evaluation of the mean concentrations.

Trials	$\overline{O_t}$	MB	NMB	RMSE	NMSE	IOA	FAC2
All cases (B-L)	5.6	-0.2	-0.03	4.5	0.7	0.88	72%

A scatter plot was then drawn to help the reading of the results (Figure 3): it reports the simulated values (y-axis) of C_m, plotted towards the field data (x-axis). The bisector (1:1), representing a perfect model, and the two lines of FAC2 (1:0.5, 1:2) representing a factor of two from the perfect value, have been highlighted. The linear trendline was added, obtaining an angular coefficient of 0.7778 (showing a slight underestimation of the average concentration values by the model), an intercept of 1.066 (exhibiting fairly low bias) and a R^2 = 0.6054 (denoting a low dispersion of the data). This agreement between the average concentrations data was considered better than acceptable.

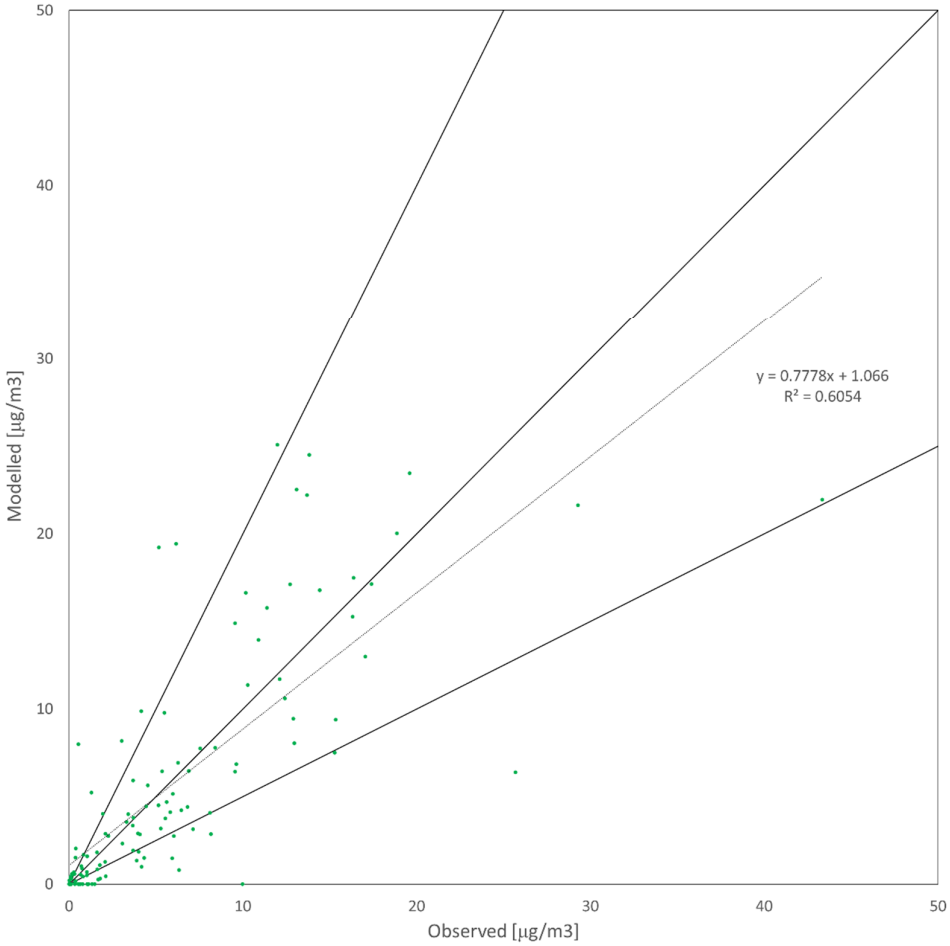

Figure 3. Scatter plot of the mean concentrations C_m. 1:1, 1:0.5, and 1:2 lines are added.

4.3. Standard Deviation of Concentration, σ_c

The results obtained from the model for the standard deviation of the concentration are shown in Figure 4. The Figure reports the simulated values (y-axis) of σ_c, plotted towards the field data (x-axis). It should be reported that, in certain experiments, the modelled values at the fast-response detector locations of the mean concentration are equal to 0. For this reason, the standard deviation is forced to 0 by the model. In the graph of Figure 3, only nonzero values are shown. The bisector line 1:1, the 1:0.5, and the 1:2 lines are also graphed. It is possible to note that 60% of all the points are within the FAC2

range. The linear trendline was added, obtaining an angular coefficient of 3.14 (showing a relevant overestimation of the standard deviation by the model), an intercept of −6.19 (exhibiting negative bias) and a $R^2 = 0.3$ (denoting a moderate linear relationship).

It is important to make some considerations regarding this comparison. The modelled standard deviation of concentration theoretically represents the standard deviation of the instantaneous sequence of concentration data. On the contrary, the experimental standard deviation, brought as a comparison to the model, is far from instantaneousness. This is the result of a not-instantaneous data sampling time (10 s) and the non-ideality of the measurement tool. For this reason, it suffers two kind of data losses: low frequency losses due to the finite mediation time and high frequency losses due to the analyzer's response time. The measured standard deviation of the concentration is forced to decrease. The overestimation of the model presented is therefore someway expected.

Despite these "Signal theory" dissertations, considering the simplicity of the model, the modelled data are considered acceptable.

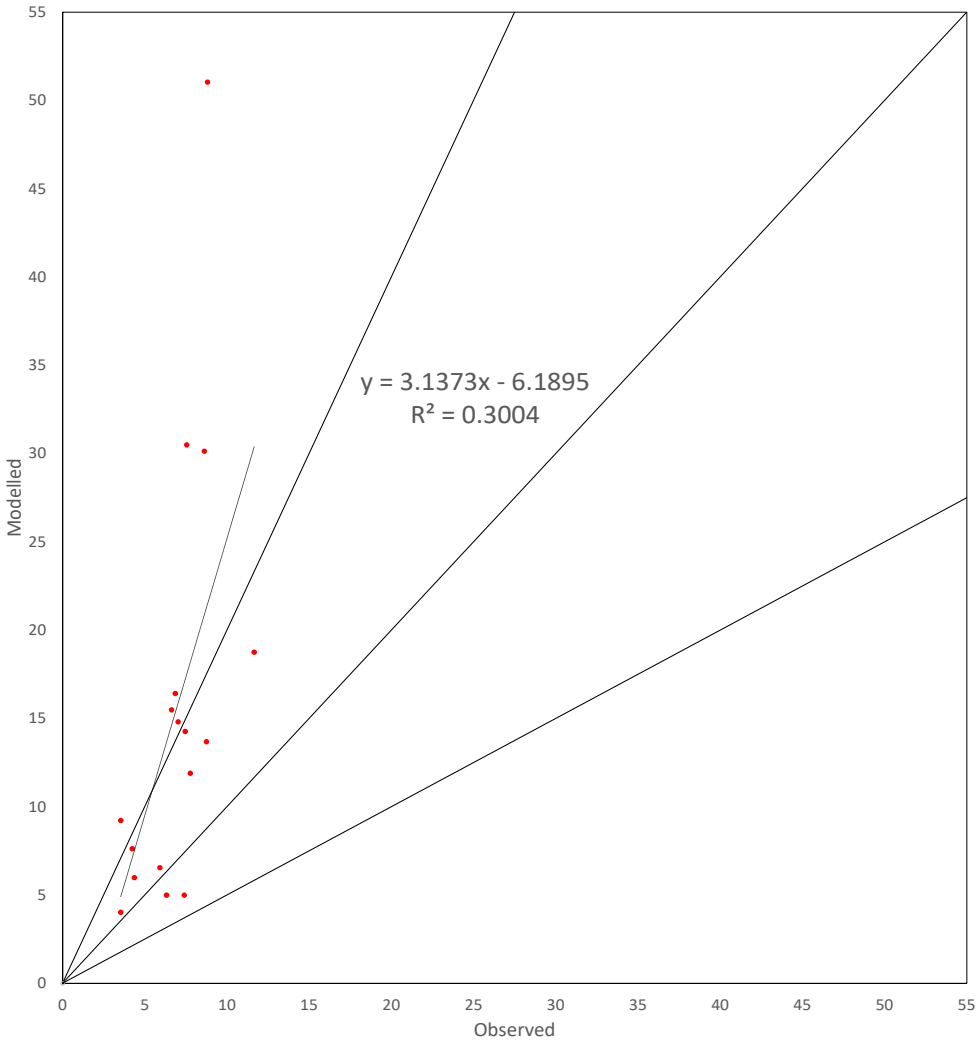

Figure 4. Scatter plot of observed against modelled σ_c (μg/m^3). Moreover, 1:1, 1:0.5, and 1:2 and trend lines are reported.

4.4. Intensity of Concentration, I_c

Figure 5 reports the simulated values (y-axis) of I_c, graphed towards the field data (x-axis). For the reason mentioned above, also in this graph the comparative points are reported only for the not-null calculated concentration intensity. The bisector line 1:1, the 1:0.5, and the 1:2 lines are also reported. It is possible to see that 40% of the value is within the range of the FAC2. Then, the linear trendline was added, obtaining an angular coefficient of 0.71, an intercept of 1.87 and a R^2 = 0.11. The correlation coefficient of 0.33 indicates a moderate linear relationship.

Remembering that the intensity of concentration is the ratio between the standard deviation of concentration and the mean concentration (see Equation (5)), it is possible to highlight that the biased behavior of overestimation of the standard deviation propagates to intensity of concentration.

It appears that the model does not perfectly describe the physical phenomenon, but the value of FAC2 is not poor considering the simplification of the model.

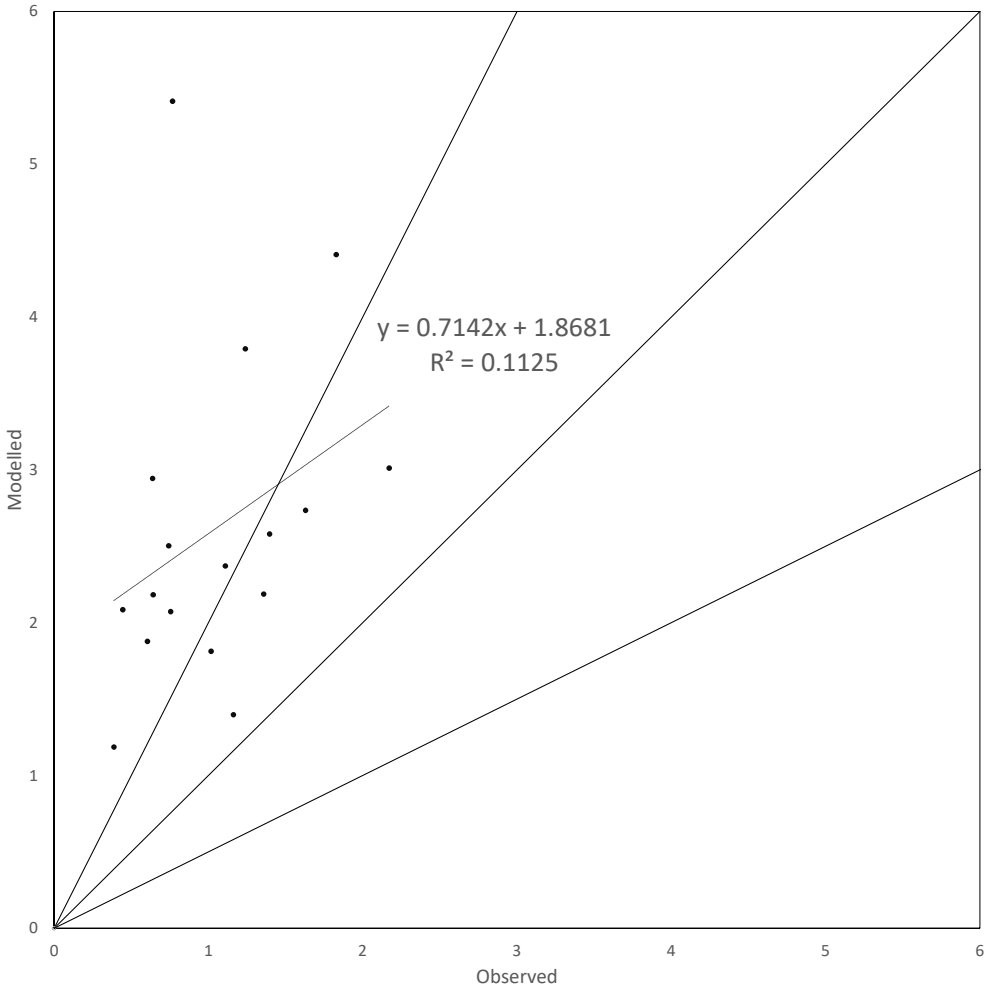

Figure 5. Scatter plot of observed against modelled I_c. Moreover, 1:1, 1:0.5, and 1:2 and trend lines are reported.

4.5. Peak-to-Mean Factor, R_{90}

The R_{90} was calculated considering both the Gamma and the Modified Weibull [83] as representative PDF for the instantaneous ambient concentration. In Figure 6, the results for the peak-to-mean factor are reported. The orange results refer to the Gamma PDF and

the blue ones to the Modified Weibull. It is possible to see the simulated values (y-axis) of R_{90} plotted in ordinate towards the field data (x-axis). On Figure 6a the scatter plot is reported. In addition to the bisector, the 1:0.5 and 1:2 lines have been reported. 90% of the results obtained by the Gamma PDF are within the range of FAC2. Instead, 80% of the results obtained with the Modified Weibull are within the FAC2 range. Focusing on the numerical indexes, in the case of the Gamma PDF, MB = 0.35, NMB = 0.15 and NMSE = 0.28 were obtained. Considering the Modified Weibull, MB = 0.87, NMB = 0.37 and NMSE = 0.79 are calculated. All the calculated correlation indexes are reported in Table 5. Because of the presence of the factor 1.5 (see Equation (21)), present in the Modified Weibull, the results for this PDF show higher values. On Figure 6b a q-q plot is reported. The results do not lay strictly on the bisector, but very similar trends can be seen for both PDFs: the obtained data seem to be diverse only for a static translation, probably due to the presence of the "safety factor" 1.5 [97].

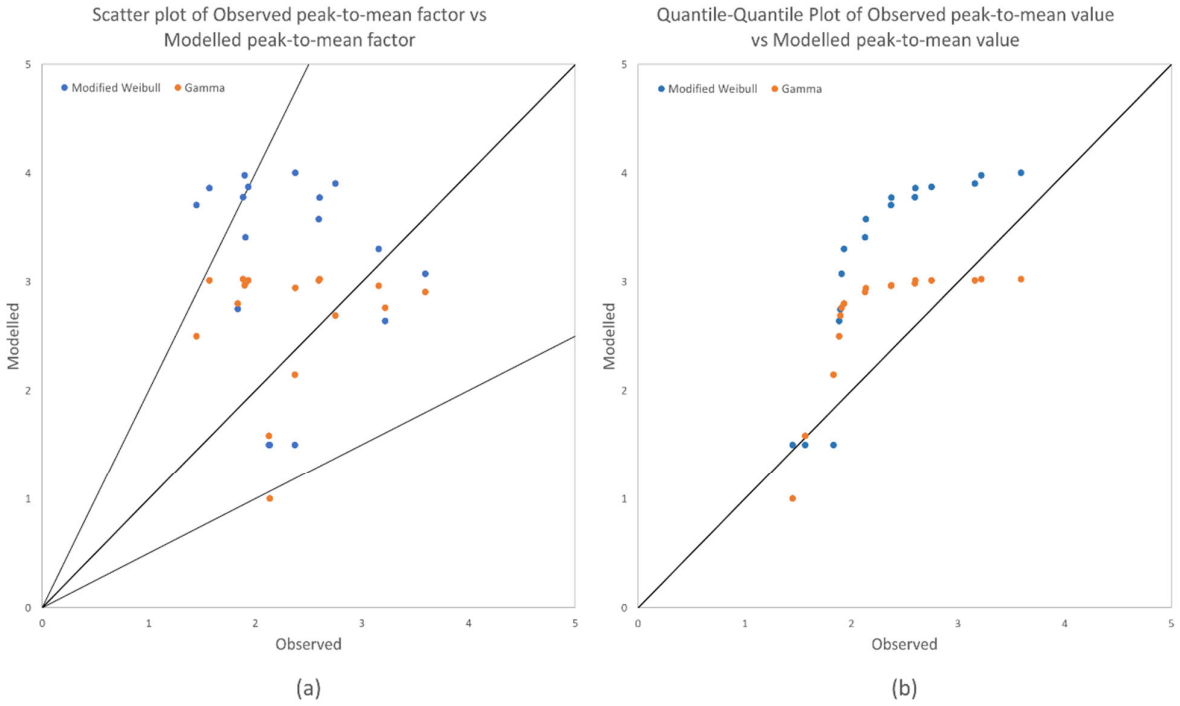

Figure 6. Peak-to-mean factor graph: (**a**) Scatter plot and (**b**) quantile–quantile plot. Moreover, 1:1 line in each graph is reported and 1:0.5 and 1:2 lines are added in the scatter plot.

Table 5. Parameters for the performance evaluation of the R_{90} obtained with the two different PDFs here considered: Gamma and Modified Weibull.

PDF	MB	NMB	RMSE	NMSE	IOA	FAC2
Gamma	0.35	0.15	0.84	0.28	0.47	94%
Modified Weibull	0.87	0.37	1.41	0.79	0.32	82%

In Figure 7, the predicted R_{90} contour plots calculated testing the Gamma PDF are shown for all considered trials, while in Figure 8 the predicted R_{90} contour plots calculated testing the Modified Weibull. Even in these graphs, it is clear that the values calculated using the Modified Weibull are higher than those obtained with the Gamma PDF as a reference. Figures 7 and 8 provide further information with respect to the scatter plot and q-q plot. It is possible to see that the values of R_{90} vary along the plumes. Not precisely at the emission source (located in the domain center) but in the strict proximity, there are higher R_{90} values (yellow-orange areas). This result depicts a different trend with respect

to the one proposed by empirical peak-to-mean literature [17,22]. They proposed a monotonic trend for the peak-to-mean value, maximum at the emission and decreasing with the downwind distance. Here-obtained results depict a non-monotonous R_{90} trend, with a peak near the source but not at the emission, then decreasing with the downwind distance, as proposed by [17,22]. This model shows a greater complexity, due to the non-unique dependence on the distance. Another observation evident from Figures 7 and 8 is that R_{90} increases with distance from the plume centerline. This evidence is in accordance with the theory of Best [98]. Referring to the cited paper, the dependency of the peak-to-mean factor from y is exponential and R_{90} increases by getting closer to the extremes of the plume, according also to experimental evidences [44,77]. Reaching the edges of the domain, the colors of the figures indicate decreasing values with distance. A characteristic shape, in certain experiments V-shape, in others Y-shape, is formed because of these dependences on x and y (lighter yellow). All these considerations are valid for both the Gamma and the Modified Weibull PDFs. It is important to note that the obtained values fall between 1 and 4, in particular 1–3 for the Gamma PDF and 1.5–4 for the Modified Weibull. More in detail, the dispersion of the points in the scatter plot for both the PDFs is evident. This can be explained by considering that the physics of the model is not completely satisfactory: there is not a monotonic trend between the simulated values of R_{90} and the experimental ones. Similar tendency of dispersion is evident also in [99], where the authors tested a new approach: the use of Lagrangian Particle Model LASAT coupled with the implementation of the concentration-variance transport and the Modified Weibull [83].

On the other hand, the q-q plot shows a tendency to the overestimation of the model with respect to the experimental values. In particular, it appears that, for both the considered PDFs, the model often provides upper limit values, which are equal to three and four for the Gamma and the Modified Weibull PDF, respectively [41]. This tendency to an asymptotic value is due to the choice to define the sub-hourly peak as the 90th percentile of the instantaneous concentration value. In fact, as mentioned in Section 2.5, the trend of R_{90} as function of I_c shows an upper limit value. As mentioned above, the obtained upper limit value depends on the hypothesized representative PDF.

Another observation can be made on the obtained peak-to-mean range: all the results fall between 1 and 4. In particular, overall-sample average peak-to-mean values have been calculated: the mean value corresponding to the Gamma PDF is 2.7; the mean value for the Modified Weibull is 3.2. Even though this represents a very rough estimation, it can be useful in order to compare it with the laws in-force.

Moreover, these values are comparable to the values obtained by using the concentration-variance transport implemented in GRAL [41,97]. In a recent paper by the authors [82], the overall time and space value for the R_{90} turned out to be equal to 2.5, which is comparable with the data here presented. Despite the points of the scatter plot (Figure 6a) exhibit quite dispersed data, it is important to note that the range of obtained R_{90} appears reasonably narrow.

As reported diffusely in the scientific literature [41,100,101], the German constant peak-to-mean value, set equal to 4 [36], appears to be rather conservative: this value represents the upper limit value for the R_{90} obtained by considering the Modified Weibull PDF. With regard to the most recently investigated value [82] used in Italian regulations, equal to 2.3 [38–40], this shows a more halfway behaviour, laying amid the obtained calculated and experimental value.

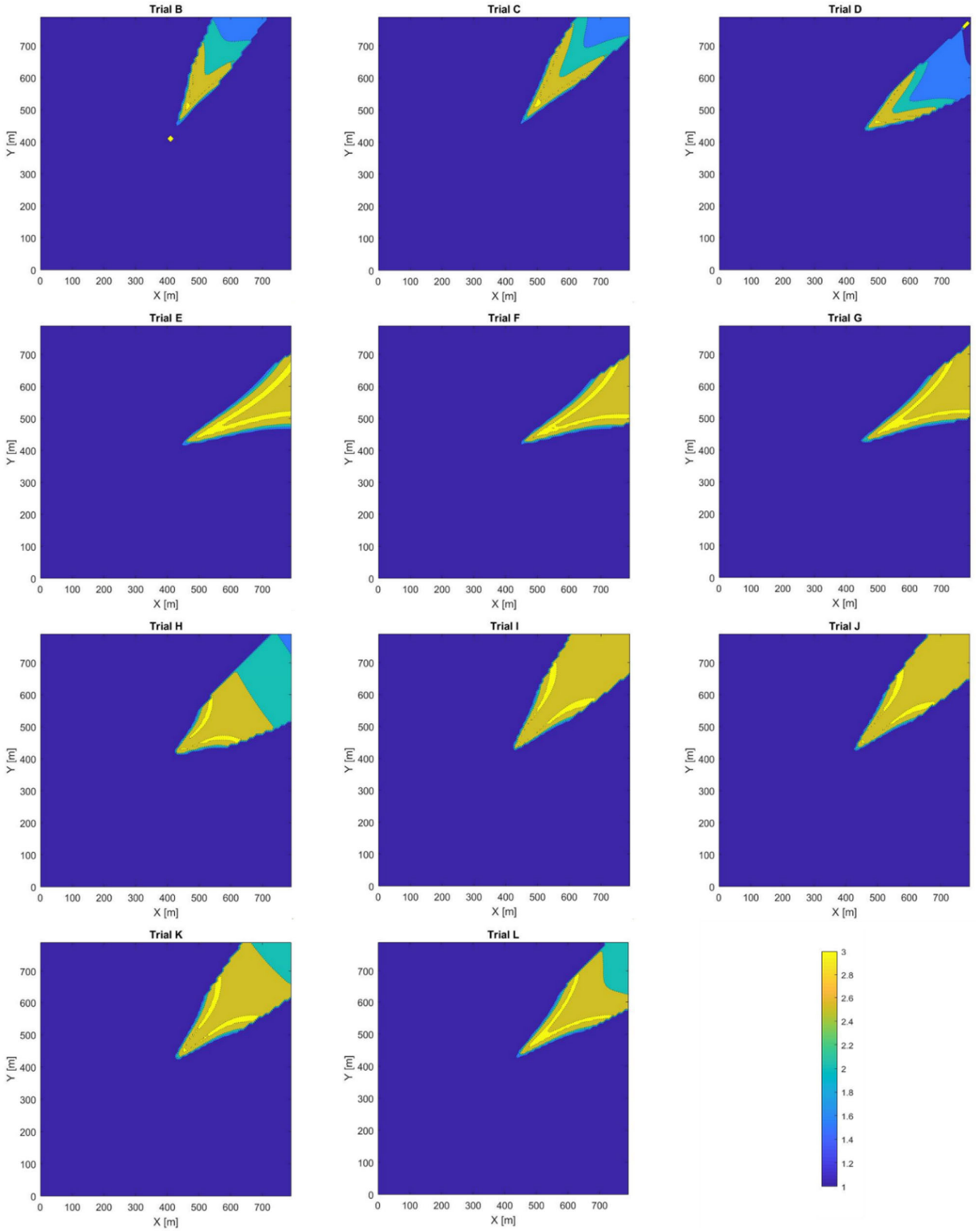

Figure 7. Modelled R_{90} contour plots using the Gamma PDF, for every trial considered. Values are ranged from 1 to 3.

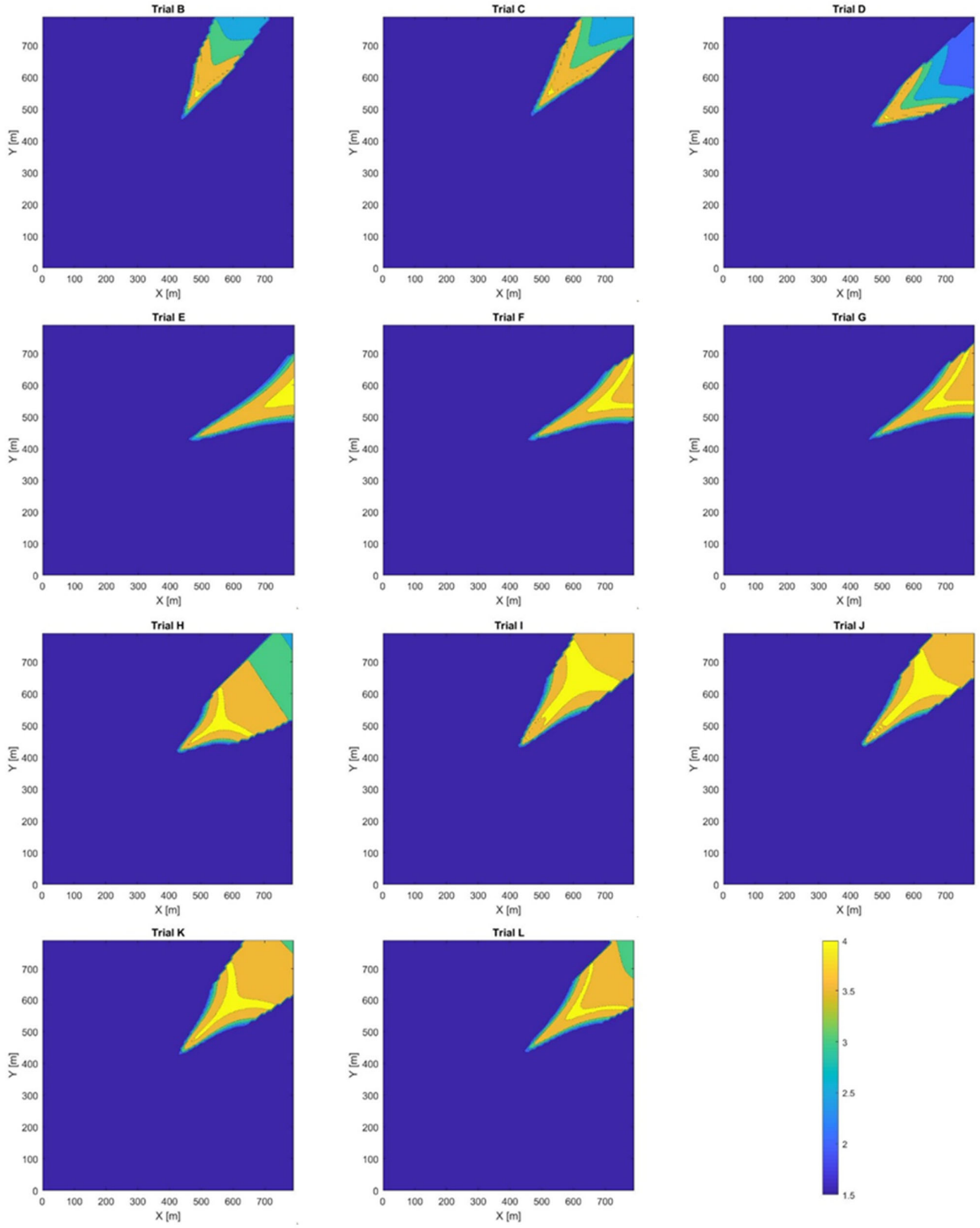

Figure 8. Modelled R_{90} contour plots using the Modified Weibull PDF, for every trial considered. Values are ranged from 1.5 to 4.

4.6. Experimental Underestimation of Peak-to-Mean

It is necessary to compare the modelling outputs with the experimental evidence reported in the literature. This comparison hides a tricky problem. The measurements obtained experimentally consist of concentration measurements produced by the various analyzers with a generic "high-frequency", whose dynamic characteristics are not usually reported in a clear and exhaustive way. From these data, the concentration intensities and P/M ratios are deduced. It would therefore seem that, with few exception [44], concentration intensities and P/M ignore any possible correction that takes into account the filtering effect of the other frequencies. These measurements are produced by an analyzer, which in general, follows a first order linear system with characteristic time τ [102]. Due to this, as shown in the micrometeorological and agrometeorological literature [91,103–106], also the sample variance produced by the analyzers at the basis of the sample estimation of concentration intensity and P/M is a clear underestimation of the real variance, theoretically obtainable with an ideal concentration measurement tool (i.e., with a null response time). The ratio between the two variances (sample and real) in stable situations can reach very high values. Therefore, the sample variance, produced by analyzers, far from truly being "fast", is an underestimation of the real variance. From this, the intensity of concentration is also an underestimation of reality. This problem also has consequences in the calculation of P/M. The experimental evidence and the PDFs taken as a model of the statistics of a passive gas in the Surface Layer clearly show that there is a relationship between concentration intensity and P/M. It presents a maximum and this prevents us from saying a priori whether the spectral losses accumulated in the estimation of the variance eventually lead to an underestimation or an overestimation of the P/M. Therefore, regarding the values of P/M found in the literature, there is an associated an intrinsic positive or negative uncertainty that is difficult to be quantified, in the light of the few or non-existent information related to the analyzers used by various authors. This makes it difficult to make a comparison with the modelling outputs that, if the physical and theoretical basis are correct and complete, can only produce estimations to which no-intrinsic uncertainty can be associated.

5. Conclusions

Atmospheric dispersion modelling has a key role in the study of environmental odors. Unlike the study of macro-pollutants, for odor impact assessment, the calculation of the short-term peak odor concentrations is fundamental. For this purpose, in this article a simplified and analytical Fluctuating Plume Model [54] is tested. It is fundamental to point out the merits of this model: it is very simple, and the equations of the mean and variance concentration can be worked out analytically. This model was here used to verify if it can provide reliable data, not only for the mean concentration, but also for σ_C, I_c and R_{90}. Moreover, for the calculation of the peaks, PDFs are necessary: Gamma and Modified Weibull PDFs were tested here. Different conclusions can be drawn from the present work.

The difficultly of Gaussian models to consider the horizontal meandering that is naturally present in nature was corroborated. For the scope of this work, wind direction data were tuned in order to fit the plume transversal limits. Seventy-two percent of the simulated mean concentration values fell within the range of the FAC2 with respect to the experimental ones. Good results are also obtained looking at the linear regression line. Moreover, the model here presented and developed, has the aim to calculate concentration variance, in order to use it for the estimation of the peak-to-mean factor R_{90}. Both the results for σ_C and I_c provide an overestimation of the experimental data. This result is strictly linked with the data losses due to the non-ideality of the measurement system: the non-theoretically instantaneous sampling (0.1 Hz) and the response time τ contribute to the flattening of the instant concentration data and so cause a decrease of the sample variance.

The propagation of the errors from I_c data to R_{90} is very complex due to the introduction of the relationships of the chosen PDF. Nonetheless, the obtained data for R_{90} show a dispersed behavior with respect to the experiment, but the ranges covered are quite repeatable: the P/M obtained values are 1–3 for the Gamma PDF and 1.5–4 for the Modified Weibull PDF, with experimental values ranging from 1.4 to 3.6. This finding can be linked to the R_{90} trend with respect to I_c: depending on the PDF, different maximum values are reached: three and four for the Gamma and the Modified Weibull, respectively.

The obtained results highlight the variability of ambient odor concentration fluctuations, which cause great confusion in complaints from citizens close to industrial activities. The model here presented is theoretically designed for neutral/slightly stable situations: in this work, the comparison was made only in neutral conditions. A future perspective could be the use of different atmospheric stability situation to test this kind of analytical models. One goal is to make it usable even in less ideal conditions. On the other hand, a limitation of the work presented here, is its inapplicability in calm wind conditions: unfortunately in these conditions the Gaussian plume models are not applicable due to the mathematical formulation that requires the presence of the wind speed term in the denominator. A further crucial point that has to be taken into consideration when "high-frequency" concentration data are used: spectral losses are implicit when using non-ideal sensors. Unluckily these considerations are very scarce in the odor nuisance research field: the considerations made in this paper could be a first step for further reflections for the development of future experimental field campaigns.

In the most advanced models, the PDFs need to be evaluated in a consistent statistical way. For this reason, it is also crucial to deepen the scientific knowledge on probability density functions, which can well describe the ambient instantaneous concentration. All these adjustments for the calculation of fluctuations will allow to modify odor legislations accordingly, with the final aim of improve the quality of life of population.

Supplementary Materials: The following are available online at www.mdpi.com/2076-3417/11/8/3310/s1. The text presents some considerations about the superposition of the effects for multiple emissions.

Author Contributions: Conceptualization, M.I. and R.S.; Data curation, M.I.; Formal analysis, M.I. and R.S.; Investigation, M.I. and F.C.; Methodology, M.I. and R.S.; Project administration, S.S.; Resources, S.S.; Software, M.I.; Supervision, M.I. and S.S.; Validation, F.C.; Visualization, F.C.; Writing–original draft, F.C.; Writing–review & editing, M.I., R.S. and L.C. All authors have read and agreed to the published version of the manuscript.

Funding: This research received no external funding.

Institutional Review Board Statement: Not applicable.

Informed Consent Statement: Not applicable.

Data Availability Statement: Not applicable.

Acknowledgments: We would thank Marlon Brancher (VetMedUni) for field-data provision.

Conflicts of Interest: The authors declare no conflict of interest.

References

1. Secundo, L.; Snitz, K.; Sobel, N. The perceptual logic of smell. *Curr. Opin. Neurobiol.* **2014**, *25*, 107–115, doi:10.1016/j.conb.2013.12.010.
2. Zhou, Y.; Hallis, S.A.; Vitko, T.; Suffet, I.H. (Mel) Identification, quantification and treatment of fecal odors released into the air at two wastewater treatment plants. *J. Environ. Manag.* **2016**, *180*, 257–263, doi:10.1016/j.jenvman.2016.05.046.
3. Roveda, L.; Polvara, E.; Invernizzi, M.; Capelli, L.; Sironi, S. Definition of an Emission Factor for VOC Emitted from Italian and European Refineries. *Atmosphere (Basel).* **2020**, *11*, 564, doi:10.3390/atmos11060564.
4. Invernizzi, M.; Ilare, J.; Capelli, L.; Sironi, S. Proposal of a method for evaluating odour emissions from refinery storage tanks. *Chem. Eng. Trans.* **2018**, *68*, 49–54, doi:10.3303/CET1868009.
5. Dunlop, M.W.; Blackall, P.J.; Stuetz, R.M. Odour emissions from poultry litter–A review litter properties, odour formation and odorant emissions from porous materials. *J. Environ. Manag.* **2016**, *177*, 306–319, doi:10.1016/j.jenvman.2016.04.009.

6. Marchand, M.; Aissani, L.; Mallard, P.; Beĺine, F.; Revéret, J.P. Odour and Life Cycle Assessment (LCA) in waste management: A local assessment proposal. *Waste Biomass Valorization* **2013**, *4*, 607–617, doi:10.1007/s12649-012-9173-z.
7. Mackie, K.R.; Cooper, C.D. Landfill gas emission prediction using Voronoi diagrams and importance sampling. *Environ. Model. Softw.* **2009**, *24*, 1223–1232, doi:10.1016/j.envsoft.2009.04.003.
8. Stull, R.B. *An introduction to boundary layer meteorology*; Kluwe Academic Press: Dordrecht, The Netherlands, 1988; ISBN 978-90-277-2769-5.
9. Sorbjan, Z. *Structure of the Atmospheric Boundary Layer*; Printice Hall: Hoboken, New Jersey, 1989; ISBN 978-0138535575.
10. Monin, A.S.; Yaglom, A.M. *Statistical Fluid Mechanics: Mechanics of Turbulence*; Dover Publications: Mineola, NY, USA, 2007; Volume 1.
11. Pope, S.B. *Turbolent Flows*; Cambridge University Press: Cambridge, MA, USA, 2000.
12. Wyngaard, J.C. *Turbolence in the Atmosphere*; Cambridge University Press: Cambridge, MA, USA, 2010.
13. Seinfeld, J.H.; Pandis, S.N. *Atmospheric Chemistry and Physics: From Air Pollution to Climate Change*; John Wiley & Sons: Hoboken, NY, USA, 2016.
14. Jacobson, M.Z. *Fundamentals of Atmospheric Modeling*, 2nd ed.; Cambridge University Press: Cambridge, MA, USA, 2005.
15. Rodean, H.C. *Stochastic Lagrangian Models of Turbulent Diffusion*; Society, A.M., Ed.; Springer: Boston, MA, USA, 1996; ISBN 978-1-935704-11-9.
16. Nicell, J.A. Assessment and regulation of odour impacts. *Atmos. Environ.* **2009**, *43*, 196–206, doi:10.1016/j.atmosenv.2008.09.033.
17. Schauberger, G.; Piringer, M.; Petz, E. Diurnal and annual variation of the sensation distance of odour emitted by livestock buildings calculated by the Austrian odour dispersion model (AODM). *Atmos. Environ.* **2000**, *34*, 4839–4851, doi:10.1016/S1352-2310(00)00240-5.
18. Invernizzi, M.; Capelli, L.; Sironi, S. Proposal of odor nuisance index as urban planning tool. *Chem. Senses* **2017**, *42*, 105–110, doi:10.1093/chemse/bjw103.
19. Palmiotto, M.; Fattore, E.; Paiano, V.; Celeste, G.; Colombo, A.; Davoli, E. Influence of a municipal solid waste landfill in the surrounding environment: Toxicological risk and odor nuisance effects. *Environ. Int.* **2014**, *68*, 16–24, doi:10.1016/j.envint.2014.03.004.
20. Liu, Y.; Liu, Y.; Li, H.; Fu, X.; Guo, H.; Meng, R.; Lu, W.; Zhao, M.; Wang, H. Health risk impacts analysis of fugitive aromatic compounds emissions from the working face of a municipal solid waste landfill in China. *Environ. Int.* **2016**, *97*, 15–27, doi:10.1016/j.envint.2016.10.010.
21. Sucker, K.; Both, R.; Winneke, G. Review of adverse health effects of odours in field studies. *Water Sci. Technol.* **2009**, *59*, 1281–1289, doi:10.2166/wst.2009.113.
22. Schauberger, G.; Piringer, M.; Schmitzer, R.; Kamp, M.; Sowa, A.; Koch, R.; Eckhof, W.; Grimm, E.; Kypke, J.; Hartung, E. Concept to assess the human perception of odour by estimating short-time peak concentrations from one-hour mean values. Reply to a comment by Janicke et al. *Atmos. Environ.* **2012**, *54*, 624–628, doi:10.1016/J.ATMOSENV.2012.02.017.
23. Klein, P.M.; Young, D.T. Concentration fluctuations in a downtown urban area. Part I: Analysis of Joint Urban 2003 full-scale fast-response measurements. *Environ. Fluid Mech.* **2011**, *11*, 23–42, doi:10.1007/s10652-010-9194-8.
24. Pope, S.B. PDF methods for turbulent reactive flows. *Prog. Energy Combust. Sci.* **1985**, *11*, 119–192, doi:10.1016/0360-1285(85)90002-4.
25. Bell, A.G. *Discovery and Invention*; Judd & Detweiler Inc.: Washington, DC, USA, 1914.
26. Bax, C.; Sironi, S.; Capelli, L. How Can Odors Be Measured? An Overview of Methods and Their Applications. *Atmosphere (Basel).* **2020**, *11*, 92.
27. Conti, C.; Guarino, M.; Bacenetti, J. Measurements techniques and models to assess odor annoyance: A review. *Environ. Int.* **2020**, *134*, 105261, doi:10.1016/J.ENVINT.2019.105261.
28. Sozzi, R. *La Micrometeorologia e La Dispersione Degli Inquinanti in Aria*; Consorzio AGE: Rome, Italy, 2003.
29. Badach, J.; Kolasińska, P.; Paciorek, M.; Wojnowski, W.; Dymerski, T.; Gębicki, J.; Dymnicka, M.; Namieśnik, J. A case study of odour nuisance evaluation in the context of integrated urban planning. *J. Environ. Manag.* **2018**, *213*, 417–424, doi:10.1016/j.jenvman.2018.02.086.
30. Danuso, F.; Rocca, A.; Ceccon, P.; Ginaldi, F. A software application for mapping livestock waste odour dispersion. *Environ. Model. Softw.* **2015**, *69*, 175–186, doi:10.1016/j.envsoft.2015.03.016.
31. Liu, Y.; Zhao, Y.; Lu, W.; Wang, H.; Huang, Q. ModOdor: 3D numerical model for dispersion simulation of gaseous contaminants from waste treatment facilities. *Environ. Model. Softw.* **2019**, *113*, 1–19, doi:10.1016/j.envsoft.2018.12.001.
32. Brancher, M.; Schauberger, G.; Franco, D.; De Melo Lisboa, H. Odour impact criteria in south American regulations. *Chem. Eng. Trans.* **2016**, *54*, 169–174, doi:10.3303/CET1654029.
33. Brancher, M.; Griffiths, K.D.; Franco, D.; de Melo Lisboa, H. A review of odour impact criteria in selected countries around the world. *Chemosphere* **2017**, *168*, 1531–1570, doi:10.1016/j.chemosphere.2016.11.160.
34. Cassiani, M.; Bertagni, M.B.; Marro, M.; Salizzoni, P. Concentration Fluctuations from Localized Atmospheric Releases. *Boundary-Layer Meteorol.* **2020**, *177*, 461–510, doi:10.1007/s10546-020-00547-4.
35. Ferrero, E.; Oettl, D. An evaluation of a Lagrangian stochastic model for the assessment of odours. *Atmos. Environ.* **2019**, *206*, 237–246, doi:10.1016/j.atmosenv.2019.03.004.
36. TA-Luft *Technische Anleitung Zur Reinhaltung der Luft. First General Administrative Regulation Pertaining the Federal Immission Control Act*; Federal Ministry for Environment, Nature Conservation and Nuclear Safety: Bone, Germany, 2002; p. 252.

37. Schauberger, G.; Piringer, M. Assessment of separation distances to avoid odour annoyance: Interaction between odour impact criteria and peak-to-mean factors. *Chem. Eng. Trans.* **2012**, *30*, 13–18, doi:10.3303/CET1230003.
38. Regione Piemonte D.g.r. 9 Gennaio 2017, n. 13-4554. L.R. 43/2000-Linee Guida Per la Caratterizzazione e il Contenimento Delle Emissioni in Atmosfera Provenienti Dalle Attività ad Impatto Odorigeno. Available online: http://www.regione.piemonte.it/governo/bollettino/abbonati/2017/05/attach/dgr_04554_930_09012017.pdf (accessed on 26 February 2021).
39. Trentino Alto Adige, G. provinciale Linee Guida Per la Caratterizzazione, L'analisi e la Definizione dei Criteri Tecnici E Gestionali per la Mitigazione Delle Emissioni Delle Attività ad Impatto Odorigeno. Available online: https://www.ufficiostampa.provincia.tn.it/content/download/38536/643559/file/Linee_guida_odori.pdf (accessed on 26 February 2021).
40. Regione Lombardia D.g.r. 15 Febbraio 2012-n. IX/3018-Determinazioni Generali in Merito Alla Caratterizzazione Delle Emissioni Gassose in Atmosfera Derivanti da Attività a Forte Impatto Odorigeno. Available online: https://www.regione.lombardia.it/wps/wcm/connect/8c3b2bab-5c37-4a55-8397-b0a9d684f094/DGR+3018_2012.pdf?MOD=AJPERES&CACHEID=8c3b2bab-5c37-4a55-8397-b0a9d684f094 (accessed on 26 February 2021).
41. Oettl, D.; Ferrero, E. A simple model to assess odour hours for regulatory purposes. *Atmos. Environ.* **2017**, *155*, 162–173, doi:10.1016/j.atmosenv.2017.02.022.
42. Smith, M. *Recommended Guide for the Prediction of the Dispersion of Airborne Effluents*; No, 68-31123; American Society of Mechanical Engineers: New York, NY, USA, 1973.
43. Schauberger, G.; Schmitzer, R.; Kamp, M.; Sowa, A.; Koch, R.; Eckhof, W.; Eichler, F.; Grimm, E.; Kypke, J.; Hartung, E. Empirical model derived from dispersion calculations to determine separation distances between livestock buildings and residential areas to avoid odour nuisance. *Atmos. Environ.* **2012**, *46*, 508–515, doi:10.1016/j.atmosenv.2011.08.025.
44. Mylne, K.R.; Mason, P.J. Concentration fluctuation measurements in a dispersing plume at a range of up to 1000 m. *Q. J. R. Meteorol. Soc.* **1991**, *117*, 177–206, doi:10.1002/qj.49711749709.
45. Hoinaski, L.; Franco, D.; de Melo Lisboa, H. Comparison of plume lateral dispersion coefficients schemes: Effect of averaging time. *Atmos. Pollut. Res.* **2016**, *7*, 134–141, doi:10.1016/j.apr.2015.08.004.
46. Hoinaski, L.; Franco, D.; de Melo Lisboa, H. An analysis of error propagation in AERMOD lateral dispersion using Round Hill II and Uttenweiller experiments in reduced averaging times. *Environ. Technol.* **2017**, *38*, 639–651, doi:10.1080/09593330.2016.1205672.
47. Ferrero, E.; Manor, A.; Mortarini, L.; Oettl, D. Concentration Fluctuations and Odor Dispersion in Lagrangian Models. *Atmosphere (Basel).* **2019**, *11*, 27, doi:10.3390/atmos11010027.
48. Gifford, F. Statistical Properties of A Fluctuating Plume Dispersion Model. *Adv. Geophys.* **1959**, *6*, 117–137, doi:10.1016/S0065-2687(08)60099-0.
49. Luhar, A.K.; Hibberd, M.F.; Borgas, M.S. A skewed meandering plume model for concentration statistics in the convective boundary layer. *Atmos. Environ.* **2000**, *34*, 3599–3616, doi:10.1016/S1352-2310(00)00111-4.
50. Cassiani, M.; Giostra, U. A simple and fast model to compute concentration moments in a convective boundary layer. *Atmos. Environ.* **2002**, *36*, 4717–4724, doi:10.1016/S1352-2310(02)00564-2.
51. Franzese, P. Lagrangian stochastic modeling of a fluctuating plume in the convective boundary layer. *Atmos. Environ.* **2003**, *37*, 1691–1701, doi:10.1016/S1352-2310(03)00003-7.
52. Mortarini, L.; Franzese, P.; Ferrero, E. A fluctuating plume model for concentration fluctuations in a plant canopy. *Atmos. Environ.* **2009**, *43*, 921–927, doi:10.1016/j.atmosenv.2008.10.035.
53. Luhar, A.K.; Sawford, B.L. Micromixing modelling of mean and fluctuating scalar fields in the convective boundary layer. *Atmos. Environ.* **2005**, *39*, 6673–6685, doi:10.1016/j.atmosenv.2005.07.047.
54. Marro, M.; Nironi, C.; Salizzoni, P.; Soulhac, L. Dispersion of a Passive Scalar Fluctuating Plume in a Turbulent Boundary Layer. Part II: Analytical Modelling. *Boundary-Layer Meteorol.* **2015**, *156*, 447–469, doi:10.1007/s10546-015-0041-9.
55. Nironi, C.; Salizzoni, P.; Marro, M.; Mejean, P.; Grosjean, N.; Soulhac, L. Dispersion of a Passive Scalar Fluctuating Plume in a Turbulent Boundary Layer. Part I: Velocity and Concentration Measurements. *Boundary-Layer Meteorol.* **2015**, *156*, 415–446, doi:10.1007/s10546-015-0040-x.
56. Bachlin, W.; Rühling, A.; Lohmeyer, A. Bereitstellung von validierungs-daten Für Geruchsausbreitungs-modelle–Naturmessungen, ingenieurbüro lohmeyer. Available online: https://pudi.lubw.de/detailseite/-/publication/28459-Bereitstellung_von_Validierungsdaten_für_Geruchsausbreitungsmodelle_-_Naturmessungen.pdf (accessed on 26 February 2021).
57. Mahrt, L.; Mills, R. Horizontal diffusion by submeso motions in the stable boundary layer. *Environ. Fluid Mech.* **2009**, *9*, 443–456, doi:10.1007/s10652-009-9126-7.
58. Anfossi, D.; Oettl, D.; Degrazia, G.; Goulart, A. An analysis of sonic anemometer observations in low wind speed conditions. *Boundary-Layer Meteorol.* **2005**, *114*, 179–203, doi:10.1007/s10546-004-1984-4.
59. Mortarini, L.; Ferrero, E.; Falabino, S.; Trini Castelli, S.; Richiardone, R.; Anfossi, D. Low-frequency processes and turbulence structure in a perturbed boundary layer. *Q. J. R. Meteorol. Soc.* **2013**, *139*, 1059–1072, doi:10.1002/qj.2015.
60. Mortarini, L.; Maldaner, S.; Moor, L.P.; Stefanello, M.B.; Acevedo, O.; Degrazia, G.; Anfossi, D. Temperature auto-correlation and spectra functions in low-wind meandering conditions. *Q. J. R. Meteorol. Soc.* **2016**, *142*, 1881–1889, doi:10.1002/qj.2796.

61. Mortarini, L.; Stefanello, M.; Degrazia, G.; Roberti, D.; Trini Castelli, S.; Anfossi, D. Characterization of Wind Meandering in Low-Wind-Speed Conditions. *Boundary-Layer Meteorol.* **2016**, *161*, 165–182, doi:10.1007/s10546-016-0165-6.
62. Sykes, R.I. Concentration fluctuations in dispersing plumes. In *Lectures on Air Pollution Modeling*; American Meteorological Society: Boston, MA, USA, 1988.
63. Yee, E.; Kosteniuk, P.R.; Chandler, G.M.; Biltoft, C.A.; Bowers, J.F. Statistical characteristics of concentration fluctuations in dispersing plumes in the atmospheric surface layer. *Boundary-Layer Meteorol.* **1993**, *65*, 69–109, doi:10.1007/BF00708819.
64. Yee, E.; Chan, R.; Kosteniuk, P.R.; Chandler, G.M.; Biltoft, C.A.; Bowers, J.F. Incorporation of internal fluctuations in a meandering plume model of concentration fluctuations. *Boundary-Layer Meteorol.* **1994**, *67*, 11–39, doi:10.1007/BF00705506.
65. Yee, E.; Wilson, D.J. A comparison of the detailed structure in dispersing tracer plumes measured in grid-generated turbulence with a meandering plume model incorporating internal fluctuations. *Boundary-Layer Meteorol.* **2000**, *94*, 253–296, doi:10.1023/A:1002457317568.
66. Peterson, H.; Lamb, B. Comparison of Results from a Meandering-Plume Model with Measured Atmospheric Tracer Concentration Fluctuations. *J. Appl. Meteor.* **1992**, *31*, 553–564.
67. Peterson, H.; Lamb, B. An Investigation of Instantaneous Diffusion and Concentration Fluctuations. *J. Appl. Meteor.* **1995**, *34*, 2724–2746.
68. Ma, Y.; Boybeyi, Z.; Hanna, S.; Chayantrakom, K. Plume dispersion from the MVP field experiment. Analysis of surface concentration and its fluctuations. *Atmos. Environ.* **2005**, *39*, 3039–3054, doi:10.1016/j.atmosenv.2005.01.008.
69. Peterson, H.; Mazzolini, D.; O'Neill, S.; Lamb, B. Instantaneous spread of plumes in the surface layer. *J. Appl. Meteorol.* **1999**, *38*, 343–352, doi:10.1175/1520-0450(1999)038<0343:ISOPIT>2.0.CO;2.
70. Yee, E.; Chan, R.; Kosteniuk, P.R.; Chandler, G.M.; Biltoft, C.A.; Bowers, J.F. Experimental measurements of concentration fluctuations and scales in a dispersing plume in the atmospheric surface layer obtained using a very fast response concentration detector. *J. Appl. Meteor.* **1994**, *33*, 996–1016.
71. Yeung, P.K.; Borgas, M.S. Relative dispersion in isotropic turbulence. Part 1. Direct numerical simulations and Reynolds-number dependence. *J. Fluid Mech.* **2004**, *503*, 93–124, doi:10.1017/S0022112003007584.
72. Yeung, P.K.; Pope, S.B. Lagrangian statistics from direct numerical simulations of isotropic turbulence. *J. Fluid Mech.* **1989**, *207*, 531–586, doi:10.1017/S0022112089002697.
73. Dosio, A.; Vilà-Guerau de Arellano, J. Statistics of absolute and relative dispersion in the atmospheric convective boundary layer: A large-eddy simulation study. *J. Atmos. Sci.* **2006**, *63*, 1253–1272, doi:10.1175/JAS3689.1.
74. Sykes, R.I.; Henn, D.S. Large-eddy simulation of concentration fluctuations in a dispersing plume. *Atmos. Environ. Part A. Gen. Top.* **1992**, *26*, 3127–3144.
75. Finn, D.; Clawson, K.L.; Carter, R.G.; Rich, J.D.; Biltoft, C.; Leach, M. Analysis of Urban Atmosphere Plume Concentration Fluctuations. *Boundary-Layer Meteorol.* **2010**, *136*, 431–456, doi:10.1007/s10546-010-9510-3.
76. Lung, T.; Müller, H.-J.; Gläser, M.; Möller, B. Measurements and Modelling of Full-Scale Concentration Fluctuations. *Agrartech. Forsch.* **2002**, *8*, E5–E15.
77. Mylne, K.R. Concentration fluctuation measurements in a plume dispersing in a stable surface layer. *Boundary-Layer Meteorol.* **1992**, *60*, 15–48, doi:10.1007/BF00122060.
78. Yee, E.; Wang, B.C.; Lien, F.S. Probabilistic model for concentration fluctuations in compact-source plumes in an urban environment. *Boundary-Layer Meteorol.* **2009**, *130*, 169–208, doi:10.1007/s10546-008-9347-1.
79. Sawford, B.L. Conditional concentration statistics for surface plumes in the atmospheric boundary layer. *Boundary-Layer Meteorol.* **1987**, *38*, 209–223, doi:10.1007/BF00122445.
80. Hanna, S.R. The exponential probability density function and concentration fluctuations in smoke plumes. *Boundary-Layer Meteorol.* **1984**, *29*, 361–375, doi:10.1007/BF00120535.
81. Lewellen, W.S.; Sykes, R.I. Analysis of concentration fluctuations from lidar observations of atmospheric plumes. *J. Appl. Meteorol. Climatol.* **1986**, *25*, 1145–1154.
82. Invernizzi, M.; Brancher, M.; Sironi, S.; Capelli, L.; Piringer, M.; Schauberger, G. Odour impact assessment by considering short-term ambient concentrations: A multi-model and two-site comparison. *Environ. Int.* **2020**, *144*, 17, doi:10.1016/j.envint.2020.105990.
83. Oettl, D.; Kropsch, M.; Mandl, M. Odour assessment in the vicinity of a pig-fatting farm using field inspections (EN 16841-1) and dispersion modelling. *Atmos. Environ.* **2018**, *181*, 54–60, doi:10.1016/j.atmosenv.2018.03.029.
84. Yee, E.; Skvortsov, A. Scalar fluctuations from a point source in a turbulent boundary layer. *Phys. Rev. E Stat. Nonlinear Soft Matter Phys.* **2011**, *84*, 1–7, doi:10.1103/PhysRevE.84.036306.
85. Taylor, G. Diffusion by continuous movements. *Proc. London Math. Soc.* **1922**, 196–211, doi:10.1112/plms/s2-20.1.196.
86. Olesen, H.R.; Berkowicz, R.; Løfstrøm, P. *OML: Review of Model Formulation*; National Environmental Research Institute: Aarhus, Denmark, 2007; ISBN 1600-0048 / 978-87-7772-971-3.
87. Franzese, P.; Cassiani, M. A statistical theory of turbulent relative dispersion. *J. Fluid Mech.* **2007**, *571*, 391–417, doi:10.1017/S0022112006003375.
88. Gailis, R.M.; Hill, A.; Yee, E.; Hilderman, T. Extension of a fluctuating plume model of tracer dispersion to a sheared boundary layer and to a large array of obstacles. *Boundary-Layer Meteorol.* **2007**, *122*, 577–607, doi:10.1007/s10546-006-9118-9.
89. Deardorff, J.W.; Willis, G.E. Groundlevel concentration fluctuations from a buoyant and a non-buoyant source within a laboratory convectively mixed layer. *Atmos. Environ.* **1984**, *18*, 1297–1309.

90. Hibberd, M.F.; Sawford, B.L. A saline laboratory model of the planetary convective boundary layer. *Boundary-Layer Meteorol.* **1994**, *67*, 229–250, doi:10.1007/BF00713143.
91. Aubinet, M.; Vesala, T.; Papale, D. *Eddy Covariance: A Practical Guide to Measurement and Data Analysis*; Springer: Dordrecht, The Netherlands, 2012.
92. Chang, J.C.; Hanna, S.R. Air quality model performance evaluation. *Meteorol. Atmos. Phys.* **2004**, *87*, 167–196, doi:10.1007/s00703-003-0070-7.
93. Hanna, S.; Chang, J. Skyscraper rooftop tracer concentration observations in Manhattan and comparisons with urban dispersion models. *Atmos. Environ.* **2015**, *106*, 215–222, doi:10.1016/j.atmosenv.2015.01.051.
94. Willmott, C.J. On the validation of models. *Phys. Geogr.* **1981**, *2*, 184–194, doi:10.1080/02723646.1981.10642213.
95. Gustafson, W.I.; Yu, S. Generalized approach for using unbiased symmetric metrics with negative values: Normalized mean bias factor and normalized mean absolute error factor. *Atmos. Sci. Lett.* **2012**, *13*, 262–267, doi:10.1002/asl.393.
96. Rani Das, K. A Brief Review of Tests for Normality. *Am. J. Theor. Appl. Stat.* **2016**, *5*, 5, doi:10.11648/j.ajtas.20160501.12.
97. Pongratz, T.; Öttl, D.; Uhrner, U. Documentation of the Lagrangian Particle Model GRAL (Graz Lagrangian Model) Available online: http://lampz.tugraz.at/~gral/index.php/download (accessed on 26 February 2021).
98. Best, P.R.; Lunney, K.E.; Killip, C.A. Statistical elements of predicting the impact of a variety of odour sources. *Water Sci. Technol.* **2001**, *44*, 157–164.
99. Brancher, M.; Hieden, A.; Baumann-Stanzer, K.; Schauberger, G.; Piringer, M. Performance evaluation of approaches to predict sub-hourly peak odour concentrations. *Atmos. Environ. X* **2020**, *7*, 100076, doi:10.1016/j.aeaoa.2020.100076.
100. Piringer, M.; Knauder, W.; Petz, E.; Schauberger, G. A comparison of separation distances against odour annoyance calculated with two models. *Atmos. Environ.* **2015**, *116*, 22–35, doi:10.1016/j.atmosenv.2015.06.006.
101. Piringer, M.; Knauder, W.; Petz, E.; Schauberger, G. Determining separation distances to avoid odour annoyance with two models for a site in complex terrain. *Chem. Eng. Trans.* **2016**, *54*, 7–12, doi:10.3303/CET1654002.
102. Bendat, J.S.; Piersol, A.G. *Random Data: Analysis and Measurement Procedures*, 4th ed.; John Wiley & Sons: New York, NY, USA, 2010; ISBN 978-0-470-24877-5.
103. Moore, C.J. Frequency response corrections for eddy correlation systems. *Boundary-Layer Meteorol.* **1986**, *37*, 17–35, doi:10.1007/BF00122754.
104. Horst, T.W. A simple formula for attenuation of eddy fluxes measured with first-order-response scalar sensors. *Boundary-Layer Meteorol.* **1997**, *82*, 219–233, doi:10.1023/A:1000229130034.
105. Moncrieff, J.B.; Massheder, J.M.; De Bruin, H.; Elbers, J.; Friborg, T.; Heusinkveld, B.; Kabat, P.; Scott, S.; Soegaard, H.; Verhoef, A. A system to measure surface fluxes of momentum, sensible heat, water vapour and carbon dioxide. *J. Hydrol.* **1997**, *188–189*, 589–611, doi:10.1016/S0022-1694(96)03194-0.
106. Lee, X.; Massman, W.; Law, B. *Handbook of Micrometeorology: A Guide for Surface Flux Measurement and Analysis*; Springer: Dordrecht, The Netherlands, 2004; ISBN 978-1-4020-2265-4.